the TACSTD2 gene transduced imHCE_GDLD cells. The transduction of the wild-type TACSTD2 gene almost completely normalized the subcellular localization of the CLDN1 and CLDN7 proteins in the imHCE_GDLD. *Scale bars*: 50 μm. The immortalized corneal epithelial cell line from the GDLD patient and the immortalized corneal epithelial cell line from the normal cornea are abbreviated as imHCE_GDLD and imHCE_normal, respectively.

occurring in GDLD cornea because GDLD is a monogenic disorder caused by the biallelic loss of function mutation of the TACSTD2 gene. The imHCE_GDLD cells were transduced with the wild-type TACSTD2 gene by the lentivirus, with transduction efficiency as high as approximately 70% (Fig. 5A). The exogenous transduction of the wild-type TACSTD2 gene significantly increased the expression levels of the CLDN1 and CLDN7 proteins (Figs. 5B, 5C). The exogenously transduced wild-type TACSTD2 protein was found to be bound to the CLDN1 and CLDN7 proteins, as judged by immunoprecipitation analysis (Fig. 5D). In addition, the exogenous transduction of the wild-type TACSTD2 gene almost completely normalized the subcellular localization of the CLDN1 and CLDN7 proteins (Fig. 5E).

Discussion

In this study, we established the immortalized corneal epithelial cells from a GDLD patient by the transfection of SV40 large T antigen and hTERT genes. The cell line has high proliferation activity after their cumulative PDs exceed 100 and exhibits significant reduction of the barrier function, which is the major characteristic of corneal epithelial cells in a GDLD patient. Furthermore, the cell line exhibited decreased expression of the CLDN1 and CLDN7 proteins as well as the altered subcellular localization of these proteins, which shows good agreement with the in vivo GDLD cornea. Therefore, the established cell line, which well reflects the disease situation of the GDLD cornea, might be a good in vitro model for a GDLD cornea.

Normal human cells usually stop dividing at approximately 40 to 60 PDs, depending on several factors such as the age of their origin, the cell type, and the culture condition.[30] In general, the expansion of the life-span of a cell encounters a two-step barrier: senescence (M1) and crisis (M2).[31] The two replicative barriers have been shown to play a crucial role mainly in limiting the progress of tumorigenesis,[32] which is a life-threatening situation in most multicellular organisms. The M1 replicative barrier is known to be operated by two crucial tumor-suppressor genes: the retinoblastoma (RB) gene and the p53 gene. The nuclear Rb protein binding prevents accessibility of the transcription factor E2F to nuclear cyclins (E and A). Upon stimulation by growth factor receptor signals, the Rb protein is phosphorylated. It releases E2F, which can enable the activation of these S phase–related cyclins.[33] The M2 replicative barrier is known to be achieved by the shortening of telomeres, which might be attributable to the silencing of the hTERT gene expression in stem cells and others in the human body, with the notable exception being expression in germline cells.[24] Some virus-derived proteins such as the SV40 large T antigen and human papilloma virus E6/E7 proteins are known to bind to the RB and p53 proteins to abrogate their tumor-suppressive activity, resulting in the bypass of cells from the M1 stage.[34,35] The hTERT gene is known to be the rate-limiting factor in the telomerase activity, whereas other components of the telomerase-holoenzyme complex are known to be expressed constitutively in cells of many types.[36] Reportedly, the forced expression of only the hTERT gene was sufficient for the acquisition of telomerase activity.[37]

Several reports have described the immortalization of cells by single-gene transduction with SV40 large T antigen[29,35] or hTERT gene.[37,38] However, because each of the two replicative barriers M1 and M2 has strong inhibitive power to suppress cell expansion, it might be generally accepted that single-gene transduction with either of the two genes has markedly lower potential to achieve immortalization than that with both genes. It can be speculated that the reported immortalization by the single-gene transduction with either of the two genes might be at least partially attributable to the spontaneous repression of either or both RB and p53 gene(s), or the spontaneous activation of the endogenous hTERT gene, possibly because of gene mutation[39] or epigenetic alteration.[40] Since the starting cell number of our GDLD corneal epithelial cells was limited, we theorized that the immortalization process might fail if its efficiency was not high. Therefore, we chose to use both genes to easily overcome the M1 and M2 replicative barriers.

As for the development of a new therapy, the transduction of the wild-type TACSTD2 gene to the patient's corneal epithelial cells can be a promising therapy because GDLD is a monogenic disorder caused by the biallelic loss of function mutation of the TACSTD2 gene. Therefore, the transduction of the wild-type TACSTD2 gene might normalize the disease situation in the GDLD corneal epithelial cells. However, before the clinical application of the gene therapy, several issues must be resolved. Physicians must ascertain the optimal dosage of the transduced gene because, in general, faint expression would have little therapeutic effect, although overexpression might engender unanticipated side effects. For the TACSTD2 gene, overexpression of the gene might present a risk for tumorigenesis because the gene is presumably oncogenic.[41] We performed a preliminary experiment as for the gene therapy of GDLD. Approximately 70% imHCE_GDLD cells were transduced with the wild-type TACSTD2 gene. The gene transduction normalized the disease situation of corneal epithelial cells of GDLD, with increased expression of the CLDN1 and 7 proteins and altered subcellular localization of the two proteins from cytoplasm to plasma membrane. Unfortunately, after multiple repetitions of experiments, which yielded all of these promising data, we were unable to obtain the normalization of TER, perhaps because of the insufficiency of the transduction efficiency. Direct gene correction by artificial nucleases such as zinc finger nuclease and TAL effector nuclease presents another avenue for gene therapy.

In summary, the results of this study demonstrate the establishment of an immortalized corneal epithelial cell line from this GDLD patient. Currently, we are only halfway along in our understanding of GDLD pathophysiology. Moreover, no single prominent advance has occurred during the last decade in the development of novel effective treatments for GDLD. We hope that this newly established cell line will help foster breakthroughs in the examination of these important issues.

Acknowledgments

The authors thank John Bush for his excellent help in the preparation of the manuscript. We also thank the staff members at the Northwest Lions Eye Bank Foundation for helping us obtain the fresh human cornea used for this study.

Supported by Grant-in-Aid 21592238 from the Japanese Ministry of Education, Culture, Sports, Science and Technology and Grant H23-Nanchi-Ippan-084 from the Japanese Ministry of Health, Labour and Welfare. This work was also supported by research funds from the Kyoto Foundation for the Promotion of Medical Science. The authors alone are responsible for the content and writing of the paper.

Disclosure: **K. Kitazawa**, None; **S. Kawasaki**, None; **K. Shinomiya**, None; **K. Aoi**, None; **A. Matsuda**, None; **T. Funaki**, None; **K. Yamasaki**, None; **M. Nakatsukasa**, None; **N. Ebihara**, None; **A. Murakami**, None; **J. Hamuro**, None; **S. Kinoshita**, None

References

1. Nakaizumi G. A rare case of corneal dystrophy. *Acta Soc Ophthalmol Jpn*. 1914;18:949–950.
2. Gartry DS, Falcon MG, Cox RW. Primary gelatinous drop-like keratopathy. *Br J Ophthalmol*. 1989;73:661–664.
3. Mondino BJ, Rabb MF, Sugar J, Sundar Raj CV, Brown SI. Primary familial amyloidosis of the cornea. *Am J Ophthalmol*. 1981;925:732–736.
4. Weber FL, Babel J. Gelatinous drop-like dystrophy: a form of primary corneal amyloidosis. *Arch Ophthalmol*. 1980;98:144–148.
5. Fukjiki K, Kanai A, Nakajima A. Gelatinous drop-like corneal dystrophy in Japanese population [abstract]. In: Vogel F, Sperling K, eds. *Proceedings of the 7th International Congress of Human Genetics*. Berlin, Germany: Springer-Verlag; 1986;248–249.
6. Kawano H, Fujiki K, Kanai A. Prevalence of gelatinous drop-like corneal dystrophy in Japan [in Japanese]. *Atarashii Ganka*. 1992;9:1879–1882.
7. Tsujikawa M, Kurahashi H, Tanaka T, et al. Identification of the gene responsible for gelatinous drop-like corneal dystrophy. *Nat Genet*. 1999;21:420–423.
8. Tsujikawa M, Kurahashi H, Tanaka T, et al. Homozygosity mapping of a gene responsible for gelatinous drop-like corneal dystrophy to chromosome 1p. *Am J Hum Genet*. 1998;63:1073–1077.
9. Cortina MS, Porter IW, Sugar J, de la Cruz J. Boston type I keratoprosthesis for visual rehabilitation in a patient with gelatinous drop-like corneal dystrophy. *Cornea*. 2012;31:844–845.
10. Ito M, Takahashi J, Sakimoto N. Histological study of gelatinous drop-like dystrophy following excimer laser phototherapeutic keratectomy [in Japanese]. *Nippon Ganka Gakkai Zasshi*. 2000;104:44–50.
11. Uhlig CE, Groppe M, Busse H, Saeger W. Morphological and histopathological changes in gelatinous drop-like corneal dystrophy during a 15-year follow-up. *Acta Ophthalmol*. 2010;88:e273–e274. Available at: http://onlinelibrary.wiley.com/doi/10.1111/j.1755-3768.2009.01708.x/pdf. Accessed August 8, 2013.
12. Nagataki S, Tanishima T, Sakimoto T. A case of primary gelatinous drop-like corneal dystrophy. *Jpn J Ophthalmol*. 1972;16:107–116.
13. Ohzono S, Ogawa K, Kinoshita S, Moriyama H, Manabe R. Recurrence of corneal dystrophy following keratoplasty [in Japanese]. *Rinsho Ganka*. 1984;38:747–749.
14. Shinozaki K, Yoshino K, Yamagami H, Takamura E. Histochemical examination of recurrent cornea gelatinous drop-like dystrophy [abstract]. *Invest Ophthalmol Vis Sci Suppl*. 1996;37:S1020.
15. Wang J, Zhang K, Grabowska D, et al. Loss of Trop2 promotes carcinogenesis and features of epithelial to mesenchymal transition in squamous cell carcinoma. *Mol Cancer Res*. 2011;9:1686–1695.
16. Alberti S, Miotti S, Stella M, et al. Biochemical characterization of Trop-2, a cell surface molecule expressed by human carcinomas: formal proof that the monoclonal antibodies T16 and MOv-16 recognize Trop-2. *Hybridoma*. 1992;11:539–545.
17. Ripani E, Sacchetti A, Corda D, Alberti S. Human Trop-2 is a tumor-associated calcium signal transducer. *Int J Cancer*. 1998;76:671–676.
18. Nakatsukasa M, Kawasaki S, Yamasaki K, et al. Tumor-associated calcium signal transducer 2 is required for the proper subcellular localization of claudin 1 and 7: implications in the pathogenesis of gelatinous drop-like corneal dystrophy. *Am J Pathol*. 2010;177:1344–1355.
19. Fradet Y, Cordon-Cardo C, Thomson T, et al. Cell surface antigens of human bladder cancer defined by mouse monoclonal antibodies. *Proc Natl Acad Sci U S A*. 1984;81:224–228.
20. Weiss JS, Moller HU, Lisch W, et al. The IC3D classification of the corneal dystrophies. *Cornea*. 2008;27(suppl 2):S1–S83.
21. Kawasaki S, Kinoshita S. Clinical and basic aspects of gelatinous drop-like corneal dystrophy. *Dev Ophthalmol*. 2011;48:97–115.
22. Yamasaki K, Kawasaki S, Young RD, et al. Genomic aberrations and cellular heterogeneity in SV40-immortalized human corneal epithelial cells. *Invest Ophthalmol Vis Sci*. 2009;50:604–613.
23. Majo F, Rochat A, Nicolas M, Jaoude GA, Barrandon Y. Oligopotent stem cells are distributed throughout the mammalian ocular surface. *Nature*. 2008;456:250–254.
24. Kim NW, Piatyszek MA, Prowse KR, et al. Specific association of human telomerase activity with immortal cells and cancer. *Science*. 1994;266:2011–2015.
25. Mitchell JR, Wood E, Collins K. A telomerase component is defective in the human disease dyskeratosis congenita. *Nature*. 1999;402:551–555.
26. Nakayama J, Saito M, Nakamura H, Matsuura A, Ishikawa F. TLP1: a gene encoding a protein component of mammalian telomerase is a novel member of WD repeats family. *Cell*. 1997;886:875–884.
27. Feng J, Funk WD, Wang SS, et al. The RNA component of human telomerase. *Science*. 1995;269:1236–1241.
28. Scherer WF, Syverton JT, Gey GO. Studies on the propagation in vitro of poliomyelitis viruses. IV. Viral multiplication in a stable strain of human malignant epithelial cells (strain HeLa) derived from an epidermoid carcinoma of the cervix. *J Exp Med*. 1953;97:695–710.
29. Araki-Sasaki K, Ohashi Y, Sasabe T, et al. An SV40-immortalized human corneal epithelial cell line and its characterization. *Invest Ophthalmol Vis Sci*. 1995;36:614–621.
30. Hayflick L. The limited in vitro lifetime of human diploid cell strains. *Exp Cell Res*. 1965;37:614–636.
31. Wright WE, Pereira-Smith OM, Shay JW. Reversible cellular senescence: implications for immortalization of normal human diploid fibroblasts. *Mol Cell Biol*. 1989;9:3088–3092.
32. Shay JW, Wright WE, Werbin H. Defining the molecular mechanisms of human cell immortalization. *Biochim Biophys Acta*. 1991;1072:1–7.
33. Shirodkar S, Ewen M, DeCaprio JA, et al. The transcription factor E2F interacts with the retinoblastoma product and a p107-cyclin A complex in a cell cycle-regulated manner. *Cell*. 1992;68:157–166.
34. Bryan TM, Reddel RR. SV40-induced immortalization of human cells. *Crit Rev Oncog*. 1994;5:331–357.
35. Wilson SE, Weng J, Blair S, He YG, Lloyd S. Expression of E6/E7 or SV40 large T antigen-coding oncogenes in human corneal endothelial cells indicates regulated high-proliferative capacity. *Invest Ophthalmol Vis Sci*. 1995;36:32–40.
36. Weinrich SL, Pruzan R, Ma L, et al. Reconstitution of human telomerase with the template RNA component hTR and the catalytic protein subunit hTRT. *Nat Genet*. 1997;17:498–502.

37. Bodnar AG, Ouellette M, Frolkis M, et al. Extension of life-span by introduction of telomerase into normal human cells. *Science*. 1998;279:349–352.

38. Offord EA, Sharif NA, Mace K, et al. Immortalized human corneal epithelial cells for ocular toxicity and inflammation studies. *Invest Ophthalmol Vis Sci*. 1999;40:1091–1101.

39. Guimaraes DP, Hainaut P. TP53: a key gene in human cancer. *Biochimie*. 2002;84:83–93.

40. Renaud S, Loukinov D, Abdullaev Z, et al. Dual role of DNA methylation inside and outside of CTCF-binding regions in the transcriptional regulation of the telomerase hTERT gene. *Nucleic Acids Res*. 2007;35:1245–1256.

41. Wang J, Day R, Dong Y, Weintraub SJ, Michel L. Identification of Trop-2 as an oncogene and an attractive therapeutic target in colon cancers. *Mol Cancer Ther*. 2008;7:280–285.

STEM CELLS®
TISSUE-SPECIFIC STEM CELLS

Corneal Endothelial Cell Fate Is Maintained by LGR5 Through the Regulation of Hedgehog and Wnt Pathway

KANA HIRATA-TOMINAGA,[a] TAKAHIRO NAKAMURA,[a,b] NAOKI OKUMURA,[a,c] SATOSHI KAWASAKI,[a] EUNDUCK P. KAY,[c] YANN BARRANDON,[d] NORIKO KOIZUMI,[a,c] SHIGERU KINOSHITA[a]

[a]Department of Ophthalmology, Kyoto Prefectural University of Medicine, Kyoto, Japan; [b]Research Center for Inflammation and Regenerative Medicine, Doshisha University, Kyoto, Japan; [c]Department of Biomedical Engineering, Faculty of Life and Medical Sciences, Doshisha University, Kyotanabe, Japan; [d]Laboratory of Stem Cell Dynamics, Ecole Polytechnique Federale de Lausanne, Lausanne, Switzerland

Key Words. Cornea • Endothelium • Stem cell • LGR5 • Hedgehog • Wnt

ABSTRACT

Leucine-rich repeat-containing G protein-coupled receptor 5 (LGR5), a target of Wnt signaling, is reportedly a marker of intestine, stomach, and hair follicle stem cells in mice. To gain a novel insight into the role of LGR5 in human corneal tissue, we performed gain- and loss-of-function studies. The findings of this study show for the first time that LGR5 is uniquely expressed in the peripheral region of human corneal endothelial cells (CECs) and that LGR5$^{(+)}$ cells have some stem/progenitor cell characteristics, and that in human corneal endothelium, LGR5 is the target molecule and negative feedback regulator of the Hedgehog (HH) signaling pathway. Interestingly, the findings of this study show that persistent LGR5 expression maintained endothelial cell phenotypes and inhibited mesenchymal transformation (MT) through the Wnt pathway. Moreover, R-spondin-1, an LGR5 ligand, dramatically accelerated CEC proliferation and also inhibited MT through the Wnt pathway. These findings provide new insights into the underlying homeostatic regulation of human corneal endothelial stem/progenitor cells by LGR5 through the HH and Wnt pathways. STEM CELLS *2013;31:1396–1407*

Disclosure of potential conflicts of interest is found at the end of this article.

INTRODUCTION

In most vertebrates, including humans and other primates, the majority of external information is gained through eyesight, and the cornea is a very important avascular tissue related to the maintenance of this vision system. The cornea consists of a stratified surface epithelial cell layer, a thick collagenous stroma, and an inner single-cell-layered endothelium. Through the combination of these three cell layers, corneal tissue is kept optically clear, and ocular homeostasis and integrity are maintained. According to the World Health Organization, an estimated 25-million people worldwide are affected by cornea-related blindness [1]. Therefore, it is important to understand the underlying mechanisms by which corneal integrity is maintained.

From the medical standpoint, corneal endothelial cells (CECs) represent the most important component of the cornea, as they are crucial for maintaining corneal integrity [2]. CECs, which are derived from the neural crest, play an essential role in the maintenance of corneal transparency through their barrier and pump functions. Although human CECs are mitotically inactive and are arrested at the G1 phase of the cell cycle in vivo [3], they retain the capacity to proliferate in vitro [4]. However, a recent study has shown that to date, culturing human CECs for a long period of time is extremely difficult [5]. In view of these findings, it is now understood that the molecular mechanism, including the stem cell biology of corneal endothelial behavior, is an important research subject to explore to better understand the role and function of the cornea, as well as to elucidate the most effective means by which to reconstruct damaged corneal tissue.

It is well known that stem cells facilitate the maintenance of self-renewing tissues and organs [6–8]. With regard to corneal tissue, various studies indicate that corneal epithelial stem cells reside in the basal layer of the peripheral cornea in the limbal zone [9–11]. In contrast, even though it has been reported that CECs from the peripheral area of the cornea retain higher replication ability [12], the corneal endothelial stem cells have yet to be specifically identified and their exact locations are also not fully understood owing to the lack of unique markers and the absence of stem cell assay [13–15].

Recently, genetic mouse models have allowed for the visualization, isolation, and genetic marking of leucine-rich

Author contributions: K.H.-T.: provision of study material or patients, collection and/or assembly of data; T.N.: conception and design, collection and/or assembly of data, data analysis and interpretation, writing manuscript; N.O.: collection and/or assembly of data, S. KAWASAKI: collection and/or assembly of data; E.P.K.: data analysis and interpretation; Y.B.: financial support; N.K.: data analysis and interpretation; financial support; S. KINOSHITA: collection and/or assembly of data. K.H.T. and T.N. contributed equally to this article.

Correspondence: Takahiro Nakamura, M.D., Ph.D., Department of Ophthalmology, Kyoto Prefectural University of Medicine, 465 Kajii-cho, Hirokoji-agaru, Kawaramachi-dori, Kamigyo-ku, Kyoto 602-0841, Japan. Telephone: +81-75-251-5578; Fax: +81-75-251-5663; e-mail: tnakamur@koto.kpu-m.ac.jp Received September 18, 2012; accepted for publication March 4, 2013; first published online in STEM CELLS *EXPRESS* April 3, 2013. 1066-5099/2013/$30.00/0 doi: 10.1002/stem.1390

repeat G protein-coupled receptor 5 (LGR5)-positive cells and have provided evidence that there are stem cells in the stomach, small intestine, colon, and hair follicles of those mice [16–18]. LGR5 reportedly is expressed downstream of Hedgehog (HH) signaling in basal cell carcinoma, and $LGR5^{high}$ cells in hair follicles reportedly show active HH signaling [16, 19]. To gain more insights on the mechanism of corneal stem cells, we performed Affymetrix Microarray (Affymetrix, Inc., Santa Clara, CA) analyses using holoclone-type human corneal keratinocytes, and LGR5 was identified as a potential marker for human corneal keratinocyte stem/progenitor cells (data not shown). These findings have led us to an interesting hypothesis that a common stem cell marker exists between developmentally distinct tissues, yet to date, there have been no reports regarding the role and function of LGR5 in CECs.

In this study, we show for the first time that LGR5 is uniquely expressed in the peripheral region of human CECs and that $LGR5^{+}$ cells have some stem/progenitor cell characteristics. In addition, the findings of this study show that LGR5 is a key molecule for maintaining the integrity of CECs and is mainly regulated by HH and Wnt signaling. Moreover, R-spondin-1 (RSPO1), an LGR5 ligand, was found to dramatically influence the maintenance of CECs. Thus, our data provide new insights into the underlying homeostatic regulation of corneal endothelial stem/progenitor cells by LGR5.

Materials and Methods

Tissues

All human donor cornea tissues were obtained from SightLife (Seattle, WA) eye bank, and all corneas were stored at 4°C in storage medium (Optisol; Bausch&Lomb, Rochester, NY, http://www.bausch.com). A total of 80 donor corneas were used for all experiments (donor age: 61.8 ± 8.6 years (mean ± SD); mean time to preservation: 7.6 ± 5.6 hours; mean endothelial cell density: 2,757 ± 221 mm^2; mean storage time: 6.0 ± 0.9 days). All experiments were performed in accordance with the tenets set forth in the Declaration of Helsinki. Eight corneas obtained from cynomolgus monkeys (donor age: 7.1 ± 4.5 years (mean ± SD); estimated equivalent human age: 15–42 years) housed at NISSEI BILIS Co., Ltd., Koka, Japan and Eve Bioscience, Co., Ltd., Japan, respectively, were used for this study. For other research purposes, the monkeys were given an overdose of sodium pentobarbital for euthanization intravenously according to the approval by the Laboratory Animal Use and Ethics Committee of the Shiga Laboratory, NISSEI BILIS Co., Ltd. and the institutional animal care and use committee of Eve Bioscience, Co., Ltd., respectively. The corneas of the cynomolgus monkeys were harvested after confirmation of cardiopulmonary arrest by veterinarians, and were then provided for our research. All corneas were stored at 4°C in Optisol storage medium for less than 24 hours before the experiment. All animals were housed and treated in accordance with the The Association for Research in Vision and Ophthalmology Statement for the Use of Animals in Ophthalmic and Vision Research.

Antibodies and Reagents

For immunohistochemistry and flow cytometry, the following rabbit polyclonal antibodies were used: anti-C-terminal domain of human LGR5 (71143; GeneTex Inc., San Antonio, TX) and anti-ZO1 (40-2200; Zymed Laboratories Inc., South San Francisco, CA, http://www.invitrogen.com/content.cfm?pageid11356). The following mouse monoclonal antibodies were used: anti-Na^+/K^+ ATPase (05-369; EMD Millipore Corporation, Billerica, MA http://www.emdmillipore.com), anti-Ki67, and anti-β-catenin (556003, 610153; BD Biosciences, Franklin Lakes, NJ http://www.bdbiosciences.com/home.jsp). Secondary antibodies were Alexa Fluor-488 goat anti-rabbit or mouse IgG (A11034, A11029; Molecular Probes Inc., Eugene, OR, http://www.invitrogen.com/site/us/en/home/brands/Molecular-Probes.html) and Cy3 anti-mouse IgG (715-165-150; Jackson Immunoresearch Laboratories, Inc., West Grove, PA, http://www.jacksonimmuno.com). For Western blotting, the following rabbit polyclonal antibodies were used: anti-LRP6 and p-LRP6 (3395, 2568; Cell Signaling Technology, Inc., Beverly, MA, http://www.cellsignal.com). The following mouse monoclonal antibodies were used: β-catenin (BD Biosciences) and β-actin (A5441; Sigma-Aldrich, St. Louis, MO, http://www.sigmaaldrich.com). Secondary antibodies were horse radish peroxide (HRP)-conjugated anti-rabbit or mouse IgG (NA934, NA931; GE Healthcare, Piscataway, NJ, http://www.gehealthcare.com). Recombinant human sonic HH (SHH), purmorphamine, cyclopamine, and RSPOs were purchased from R&D Systems Inc. (Minneapolis, MN, http://www.rndsystems.com).

Cell Culture

The human and monkey CECs were cultured using the method of our previously reported system [2, 20–22]. Briefly, the Descemet's membrane including CECs was stripped and digested with 2 mg/ml collagenase A (Roche Applied Science, Penzberg, Germany, http://www.roche-applied-science.com) at 37°C. After incubation for 3 hours, the CECs (individual cells and cell aggregates) obtained from individual corneas were resuspended in culture medium containing Opti-MEM-I (Invitrogen), 5% fetal bovine serum (FBS), 50 μg/ml gentamicin, and 10 μM Y-27632 (Calbiochem, LA Jolla, CA) and then plated in one well of a 12-well plate coated with FNC Coating Mix (Athena Environmental Sciences, Inc., Baltimore, MD, http://www.athenaes.com). The CECs were cultured in a humidified atmosphere at 37°C in 5% CO_2. The culture medium was changed every 2 days. When cells reached subconfluence, they were rinsed in Ca^{2+} and Mg^{2+}-free phosphate-buffered saline (PBS), trypsinized with TrypLE Select (Life Technologies) for 10 minutes at 37°C, and passaged at ratios of 1:2–4.

Immunohistochemistry

Immunohistochemical studies followed our previously described method [23, 24]. Briefly, 8-μm-thin sections and whole-mount sections prepared by peeling the Descemet's membrane from cornea tissues were placed on silane-coated slides, air dried, and fixed in 100% acetone at 4°C for 15 minutes. After washing in PBS containing 0.15% TRITON X-100 surfactant (The Dow Chemical Company, Midland, MI, http://www.dow.com) at room temperature (RT, 24°C) for 15 minutes, sections were incubated with 1% bovine serum albumin (Sigma-Aldrich) at RT for 30 minutes to block nonspecific binding. Sections were then incubated with primary antibody at RT for 1 hour and washed three times in PBS containing 0.15% TRITON X-100 for 15 minutes. Control incubations were conducted with the appropriate normal mouse and rabbit IgG at the same concentration as the primary antibody, and the primary antibody for the respective specimen was omitted. The sections were then incubated with the appropriate secondary antibodies at RT for 1 hour. After being washed three times with PBS, the sections were then coverslipped using glycerol-containing propidium iodide (PI) (Nacalai Tesque, Inc., Kyoto, Japan, https://www.nacalai.co.jp), and examined under a confocal microscope (FluoView; Olympus Corporation, Tokyo, Japan, http://www.olympus.co.jp).

Table 1. Sequences for PCR and shRNA

LGR5 (NM_003667), Forward 5′-GAGGATCTGGTGAGCCTGAGAA-3′
Reverse 5′-CATAAGTGATGCTGGAGCTGGTAA-3′
SHH (NM_000193.2), Forward 5′-ACGGCCCAGGGCACCATTCT-3′
Reverse 5′-GGACTTGACCGCCATGCCCA-3′
Ptch1 (NM_000264.3), Forward 5′-TCGCTCTGGAGCAGATTTCCAAGGG-3′
Reverse 5′-GCAGTCTGGATCGGCCGGATTG-3′
Smo (NM_005631.4), Forward 5′-GTGAGTGGCATTTGTTTTGTGGGC-3′
Reverse 5′-CAGGCATTTCTGCCGGGGCA-3′
Gli1 (NM_005269.2), Forward 5′-GCCCCCATTGCCCACTTGCT-3′
Reverse 5′-TGCAGGGGACTGCAGCTCC-3′
Gli2 (NM_005270.4), Forward 5′-GGCCGCCTAGCATCAGCGAG-3′
Reverse 5′-CACCGCCAGGTTGCCCTGAG-3′
β-Actin (NM_ 001101), Forward 5′-GGACTTCGAGCAAGAGATGG-3′
Reverse 5′-ATCTGCTGGAAGGTGGACAG-3′
sh LGR5, 5′-CCGGGCTCTACTGCAATTTGGACAACTCGAGTTGTCCAAATTGCAGTAGAGCTTTTT-3′
sh NT, 5′-CCGGCAACAAGATGAAGAGCACCAACTCGAGTTGGTGCTCTTCATCTTGTTGTTTTT-3′

Abbreviations: LGR5, leucine-rich repeat G protein-coupled receptor 5; PCR, polymerase chain reaction; Ptch1, protein patched homolog one receptor molecule; SHH, sonic Hedgehog; sh NT, short hairpin nontarget; shRNA, short hairpin RNA; Smo, smoothened receptor molecule.

Real-Time Polymerase Chain Reaction

Real-time polymerase chain reaction (PCR) was performed following our previously described method [19]. To prepare the samples, we first separated the central cornea from the peripheral cornea using an 8-mm trephine. We then stripped the Descemet's membrane including CECs using micro forceps under a microscope to separate the corneal epithelium, stroma, and endothelium in the central and peripheral cornea, respectively. We then separated the corneal epithelial cells from the corneal stroma using dispase treatment (37°C for 1 hour). All samples were homogenized in lysis buffer (Buffer RLT; QIAGEN, Inc., Valencia, CA http://www.qiagen.com) and total RNA was eluted by use of the RNeasy Mini Kit (QIAGEN) according to the manufacturer's instructions. The relative abundance of transcripts was detected by use of SYBR Green PCR Master Mix (Applied Biosystems, Inc., Foster City, CA http://www.appliedbiosystems.com) according to the manufacturer's instructions. The primers that were used are shown in Table 1.

Flow Cytometry

For the cell sorting of $LGR5^{high}$ cells, monkey CECs prepared as described above were passaged in 1:2 dilutions and cultured to subconfluence. The CECs were dissociated to single cells by use of TrypLE Select. We then performed the following two experiments. First, the CECs were fixed in 70% (wt/vol) ethanol at 4°C for 2 hours, washed with PBS, and incubated at RT for 15 minutes with 1% FBS. The CECs were then incubated with 1:100-diluted anti-rabbit LGR5 and 1:100-diluted anti-mouse Ki67, washed, and incubated with 1:1500-diluted Alexa Fluor 488-conjugated goat anti- rabbit IgG (Life Technologies) and 1:1000-diluted Cy3 anti-mouse IgG (Jackson Immunoresearch Laboratories). Flow cytometric analyses were then performed with FACS Aria II (BD Biosciences).

Second, the CECs were washed with PBS, and then incubated at RT for 15 minutes with 1% FBS. They were then incubated with 1:100-diluted anti-rabbit LGR5 at RT for 20 minutes, washed, and incubated with 1:1500-diluted Alexa Fluor 488-conjugated goat anti-rabbit IgG (Life Technologies). $LGR5^{high}$ and $LGR5^{low}$ cells were isolated by use of fluorescence activated cell sorting (FACS) Aria II, and the resultant cells were then cultured on an eight-well chamber slide with poly-L-lysine (Sigma-Aldrich). After 5 days of culture, those cells were immunostained by anti-mouse Ki67 as described above, and the $Ki67^{high}$ cells in each group were then counted ($n = 4$).

Measurement of Cell Area

Each isolated cell fraction was centrifuged and resuspended in culture medium. Cells (approximately 100 cells/ml) were placed in a six-well plate and photographed under an inverted microscope. Cell areas were measured randomly (200 cells/fraction) using Scion Image software and statistically analyzed [23].

RNA Interference

Short hairpin RNA (shRNA) was purchased from Sigma-Aldrich. The *LGR5* shRNA targeted sequences and the nontarget (NT) shRNA sequences are shown in Table 1. The lentivirus plasmid DNA was transfected to the HEK293T cells along plasmid packaging plasmid mixture (MISSION Lentiviral Packaging Mix; Sigma-Aldrich) using a commercially available transfection reagent (FuGENE HD; Roche Diagnostics Corporation, Indianapolis, IN, http://www.roche-diagnostics.com). After 18 hours, the media was aspirated off and replaced with complete medium. The quantity of lentiviral particles was assessed by HIV-1 p24 Antigen ELISA (Zepto-Metrix Corp., Buffalo, NY, http://www.zeptometrix.com) according to the manufacturer's instructions.

Construction of Lentivirus Plasmid Vector for Gene Expression

For the construction of the lentivirus plasmid vector that expresses the introduced gene, *LGR5*, a commercially available lentiviral vector (pLenti6.3_V5-TOPO; Life Technologies) was used. cDNAs were amplified with a primer pair (Forward Primer: CTACTTCGGGCACCA TGGACACCT, Reverse Primer: CACATATTAATTAGAGACATGGGA) encompassing an entire coding sequence of *LGR5*, gel-purified, and then ligated into the lentivirus plasmid vector.

The expression lentivirus Production and Infection were in a modified version of our protocol used for the shRNA [25]. Briefly, the lentivirus plasmid DNA was transfected to the HEK293T cells along with the plasmid packaging plasmid mixture ViraPower Lentiviral Packaging Mix (Life Technologies) which contains pLP1, pLP2, and pLP/VSVG plasmids and FuGENE HD as the transfection reagent. After 18 hours, the media was aspirated off and replaced with complete

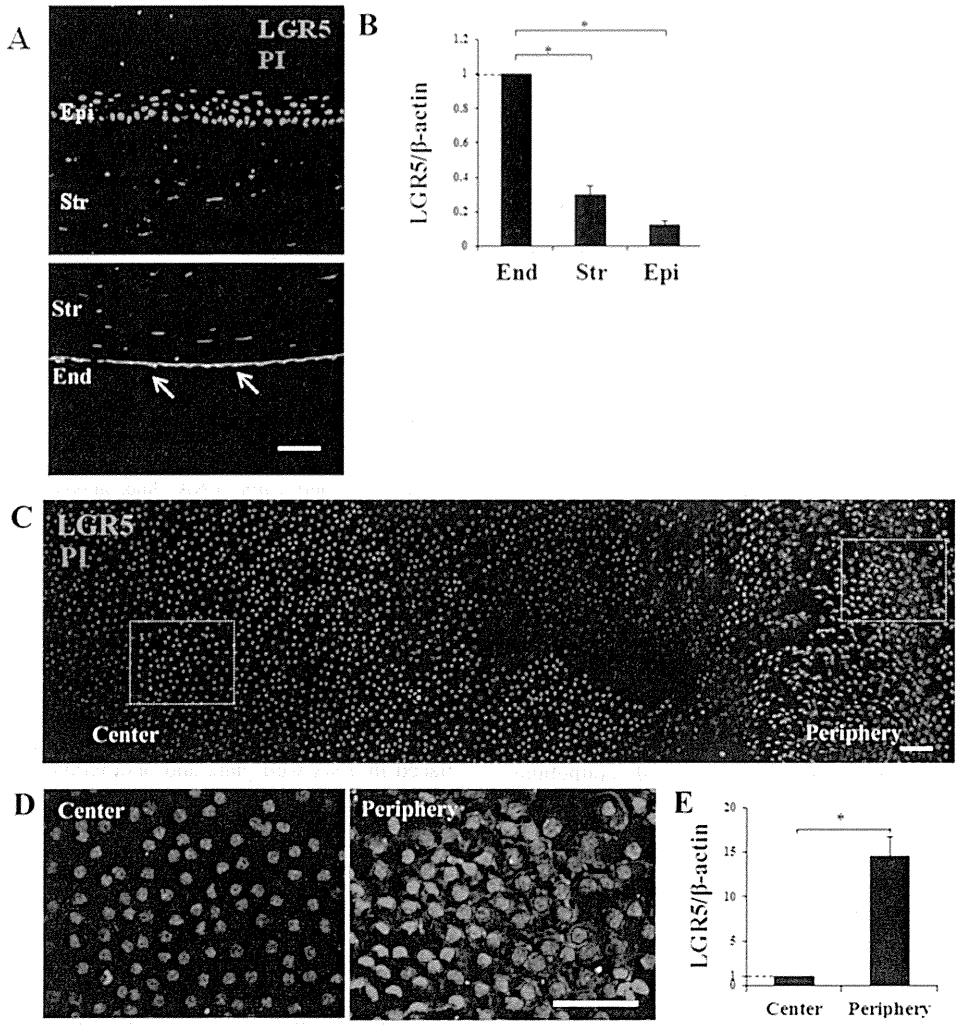

Figure 1. Unique expression pattern of leucine-rich repeat G protein-coupled receptor 5 (LGR5) in human corneal endothelial cells (CECs). **(A):** Immunostaining of LGR5 in a human cornea. Arrows point to CECs. Scale bar = 100 μm. **(B):** Real-time polymerase chain reaction (PCR) for *LGR5* in the cornea. Mean ± SEM. *, $p < .05$. $n = 4$. **(C):** Whole-mount immunostaining of LGR5 in human CECs. Scale bar = 100 μm. **(D):** Higher magnification of boxed areas in **(C)**. Scale bar = 100 μm. **(E):** Real-time PCR for *LGR5* in the central and peripheral CECs. Mean ± SEM. *, $p < .05$. $n = 3$. Abbreviations: LGR5, leucine-rich repeat G protein-coupled receptor 5; PI, propidium iodide.

medium and the quantity of lentiviral particles was then assessed.

Gene Transfer

The culture supernatant containing the infection-competent virus particle was harvested to human CECs at 5,000 cells/well in a six-well plate with FNC Coating Mix for 24 hours (Multiplicity of infection (MOI) = 1) using the culture medium described above. The supernatant was applied onto cultivated CECs in the presence of 4 μg/ml polybrene. As puromycin-resistant colonies (shRNA experiment) and blasticidin-resistant colonies (overexpression model) were collected, cells were cultured in the presence of 0.4 μg/ml of puromycin and 2 μg/ml of blasticidin, with the media being changed every 2 days.

Western Blotting

The cultivated human CECs were washed with PBS and then lysed with lysis buffer containing PBS, 1% TRITON X-100, 0.5 M EDTA, Phosphatase Inhibitor Cocktail two (Sigma-Aldrich), and Protease Inhibitor Cocktail (Roche Diagnostics). Detection of activated β-catenin (nonmembrane bound) was performed according to the previously reported protocol [26]. Briefly, cell lysates treated with Con A Sepharose 4B (GE Healthcare) were incubated at 4°C for 1 hour. After centrifugation at 4°C for 10 minutes, the supernatants were transferred to new tubes and Con A Sepharose was added to each tube and incubated at 4°C for 1 hour. Finally, after a brief centrifugation, the supernatants were transferred to new tubes and their protein concentration was determined.

The proteins were then separated by SDS polyacrylamide gel electrophoresis and transferred to polyvinylidene difluoride membranes. The membranes were then blocked with 1% ECL Advance Blocking Reagent (GE Healthcare) in Tris Buffered Saline with Tween 20 (TBS-T) buffer and were incubated with primary antibody at 4°C overnight. After being washed three times in TBS-T buffer, the polyvinylidene fluoride (PVDF) membranes were incubated with appropriate HRP-conjugated anti-rabbit or mouse IgG secondary antibody at RT for 1 hour. The membranes were exposed by use of the ECL Advance Western Blotting Detection Kit (GE Healthcare), and then examined by use of the LAS-3000 (FujiFilm Corporation, Tokyo, Japan, http://www.fujifilm.com) imaging system.

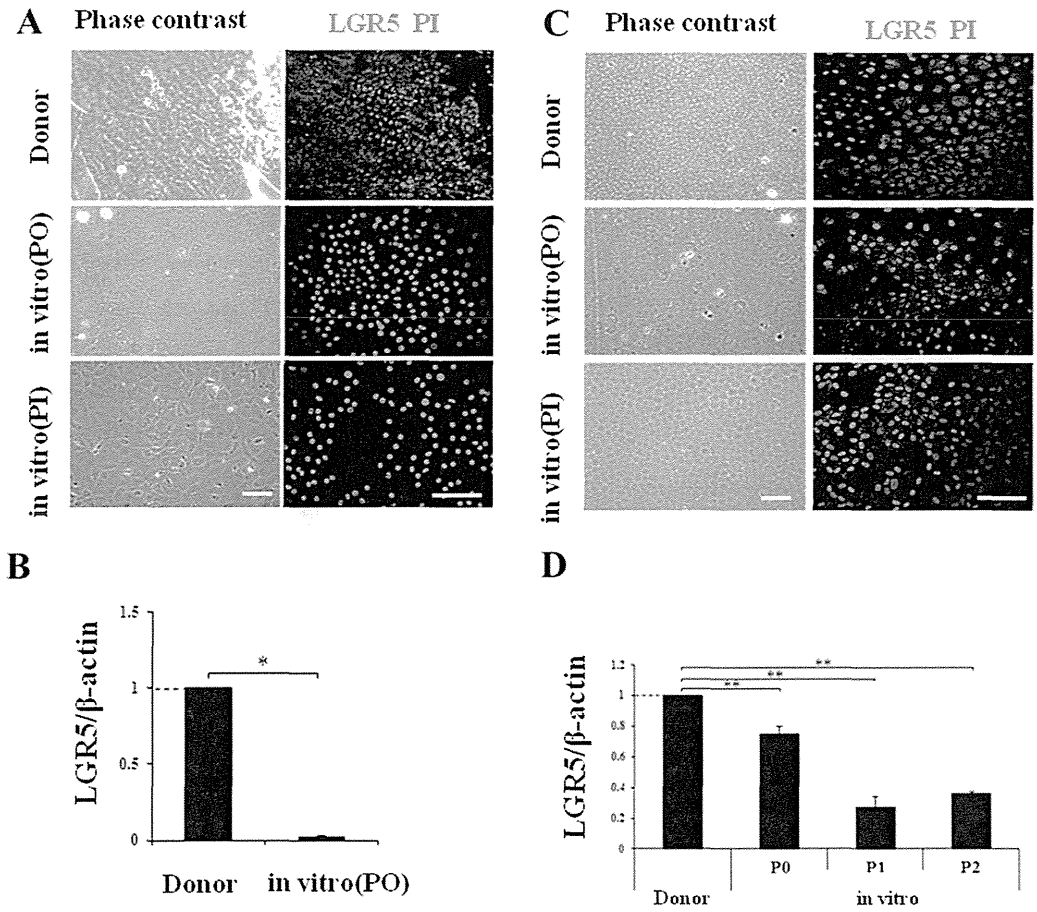

Figure 2. Downregulation of leucine-rich repeat G protein-coupled receptor 5 (LGR5) in cultivated corneal endothelial cells (CECs). **(A):** Phase contrast image and immunostaining of LGR5 in donor and in vitro human CECs. Scale bars = 100 μm. **(B):** Real-time polymerase chain reaction (PCR) for *LGR5* in donor and in vitro human CECs. Mean ± SEM. *, $p < .05$. $n = 4$. **(C):** Phase contrast image and immunostaining of LGR5 in donor and in vitro monkey CECs. Scale bars = 100 μm. **(D):** Real-time PCR for *LGR5* in donor and in vitro monkey CECs. Mean ± SEM. **, $p < .01$. $n = 3$. Abbreviations: LGR5, leucine-rich repeat G protein-coupled receptor 5; PI, propidium iodide; PO, passage 0.

Results

Unique Expression Pattern of LGR5 in Human Donor CECs

The expression pattern of LGR5 in human CECs was investigated by indirect immunofluorescence. On examination of the CECs of those tissues, intensive LGR5 expression was observed, especially in the peripheral area. However, LGR5 was only minimally expressed in the corneal epithelium and stroma (Fig. 1A). Real-time PCR showed that compared with stroma and epithelium, mean *LGR5* messenger RNA (mRNA) expression was significantly upregulated in the CECs (*$p < .05$, $n = 4$, mean age: 60 years) (Fig. 1B). Thus, among the corneal tissues, the expression of LGR5 was found to be most prominent in the CECs.

Next, we examined the location pattern of LGR5 using whole-mount immunofluorescence ($n = 3$, mean age: 64 years). The expression of LGR5 was observed in the peripheral-region CECs, yet its level gradually decreased in CECs located towards the central region (Fig. 1C, 1D). Real-time PCR clearly showed that the expression of *LGR5* in the peripheral regions was upregulated in comparison with the central region (8-mm diameter) (*$p < .05$, $n = 3$, mean age: 70 years) (Fig. 1E). These findings indicate that in corneal tissue, LGR5 is uniquely expressed in the peripheral CECs.

Downregulation of LGR5 in In Vitro Culture Conditions

It is well known that the proliferative potential of CECs varies among species [27]. To date, it is extremely difficult to consistently culture human CECs which retain a healthy morphology and high cell density. In contrast, we previously reported that under the proper in vitro conditions, monkey and rabbit CECs can proliferate reasonably well [2, 20–22]. Thus, to gain an insight into the molecular mechanism that underlies the varying proliferative potentials of CECs, we examined the expression of LGR5 in vitro.

Phase contrast microscopy photographs of human peripheral donor CECs revealed that they exhibited a confluent monolayer of smaller-size homogeneously hexagonal cells (Fig. 2A). In contrast, cultured CECs (P0, P1) were found to be enlarged and not homogeneously hexagonal (Fig. 2A). Immunostaining showed that LGR5 was well-expressed in the peripheral donor CECs (Fig. 2A). Worthy of note, the expression of LGR5 was only minimally observed in the cultured CECs in vitro (P0, P1) (Fig. 2A). Real-time PCR showed that the mean *LGR5* mRNA expression was significantly downregulated in in vitro CECs as compared to that in peripheral donor CECs (*$p < .05$) (Fig. 2B).

Phase contrast photographs of monkey CECs showed that both the peripheral donor and the in vitro (P0, P1) cells exhibited a confluent monolayer of smaller-size

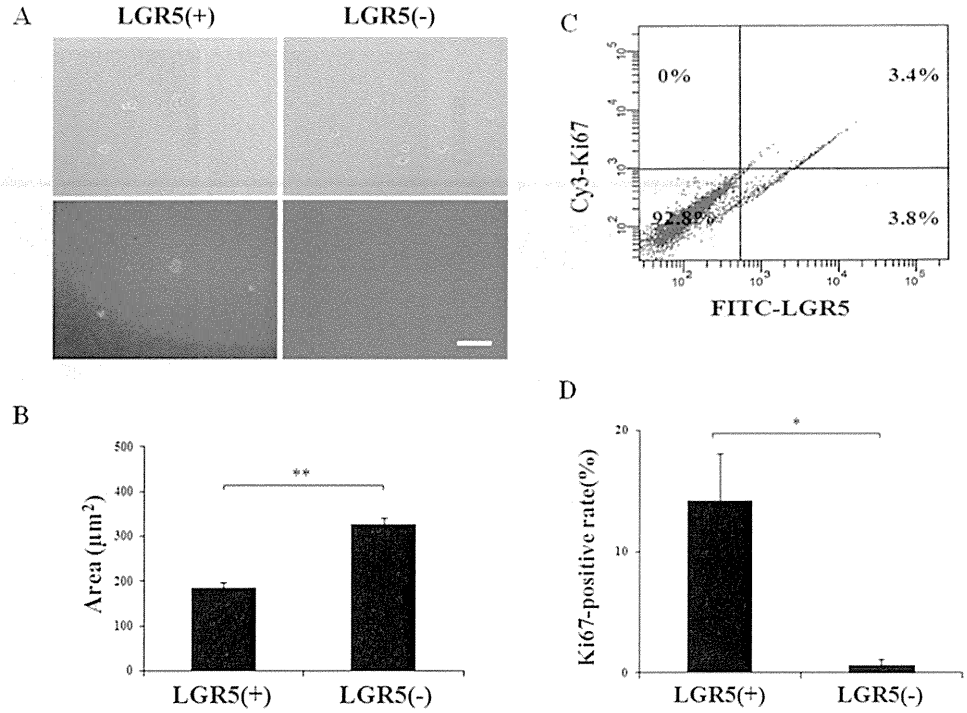

Figure 3. Characterization of leucine-rich repeat G protein-coupled receptor 5 (LGR5$^+$) Monkey corneal endothelial cells. **(A):** Phase contrast image and immunocytochemistry for LGR5 in LGR5$^+$ cells and LGR5(−) cells after cell sorting. Scale bar = 100 μm. **(B):** Average cell size of LGR5$^+$ (184.6 ± 45.8 μm^2) and LGR5$^-$ (326.78 ± 78.8 μm^2). Mean ± SEM. **, $p < .01$. $n = 35$. **(C):** Cell proliferation of LGR5$^+$ by double-immunostaining. LGR5$^+$/Ki67$^+$; 3.4%, LGR5$^+$/Ki67$^-$; 3.8%, LGR5$^-$/Ki67$^+$; 0%, LGR5$^-$/Ki67$^-$; 92.8%. **(D):** Ki67-positive rate of LGR5$^+$ and LGR5$^-$. Mean ± SEM. *, $p < .05$. $n = 4$. Abbreviations: FITC, fluorescein isothiocyanate, LGR5, leucine-rich repeat G protein-coupled receptor 5.

homogeneously hexagonal cells (Fig. 2C). The expression pattern of LGR5 in the monkey CECs closely mimicked that of in the human donor CECs (data not shown). Immunostaining of those cells showed that LGR5 is moderately expressed both in the donor cells and in vitro cells (Fig. 2C), even though the mean *LGR5* mRNA expression in vitro gradually decreased through the cell passages (*$p < .05$) (Fig. 2D). In view of these findings using human and monkey cells, it is likely that LGR5 may play a role in maintaining the cell integrity of CECs.

LGR5$^+$ CECs Were Small and Exhibited Higher Proliferative Potential

To examine the characteristics of the LGR5$^+$ and LGR5$^-$ cell fractions, the subsets were isolated by flow cytometry. To validate the cell sorting procedure, immunofluorescence for LGR5 confirmed its expression at the protein level in the purified fraction (Fig. 3A).

As the highest clonogenicity is reportedly found in the smallest keratinocytes [28], the cell size in each isolated fraction was measured by use of Scion Image software. Viewed under an inverted microscope, the LGR5$^+$ cells were found to be clearly smaller than the LGR5$^-$ cells (Fig. 3B), and the average size of the LGR5$^+$ cells was significantly smaller than that of the LGR5$^-$ cells (184.6 ± 45.8 μm^2 vs. 326.78 ± 78.8 μm^2, respectively, $n = 35$, **$p < .01$).

Next, to assess the cell-cycling status of each isolated cell fraction, FACS was used for double-staining with LGR5 and Ki67. FACS analysis showed that the LGR5^{high}/Ki67^{high} cell fraction was 3.4%, whereas the LGR5^{high}/Ki67^{low} cell fraction was 3.8% (Fig. 3C). Most interestingly, all LGR5^{low} cell fractions showed the Ki67 low level (92.8%). To further examine the proliferative capacity of each isolated cell fraction in detail, isolated cell fractions were cultivated on cell chamber slides. Five days later in culture, the percentage of Ki67-labeled cells in the LGR5$^+$ and LGR5$^-$ cells was 14.2 ± 3.87% and 0.58 ± 0.5%, respectively, rendering the difference in the Ki67-labeling index statistically significant (*$p < .05$) (Fig. 3D), suggesting that without the LGR5 expression, CECs do not have proliferative ability.

Active HH Signaling Induced LGR5 Expression

HH signaling reportedly plays a key role in various kinds of biological processes, such as cell differentiation, proliferation, and growth [16, 29, 30]. To define the properties of LGR5 in CECs at the molecular level, we first examined the expression of HH signaling-related molecules in human donor CECs. Of interest, the levels of *SHH*, *Gli1*, and *Gli2* mRNA were found to be elevated in CECs located in the peripheral-region as compared to those in the central region (Fig. 4A). On the other hand, the expression level of smoothened (*Smo*) and protein patched homolog one (*Ptch1*) receptor molecules in the HH pathway was similar (Fig. 4A). Thus, HH signaling was clearly activated in the peripheral-region CECs, suggesting that a regional variation of HH signaling activity does exist.

To determine whether the expression of LGR5 in the CECs was regulated by the HH signaling pathway, the peripheral donor CECs (outside the 8-mm central cornea area) were incubated in culture medium (Dulbecco's modified Eagle's medium + 5% FBS) and stimulated using recombinant SHH (an HH ligand, 100 ng/ml), purmorphamine (an HH agonist, 2 μM) [31], and cyclopamine (an HH antagonist, 2 μM) [32] for 24 hours at 37°C in 5% CO_2. As expected, expression of *LGR5* in the peripheral-region CECs, yet not in the central-region CECs, was found to be upregulated by SHH and

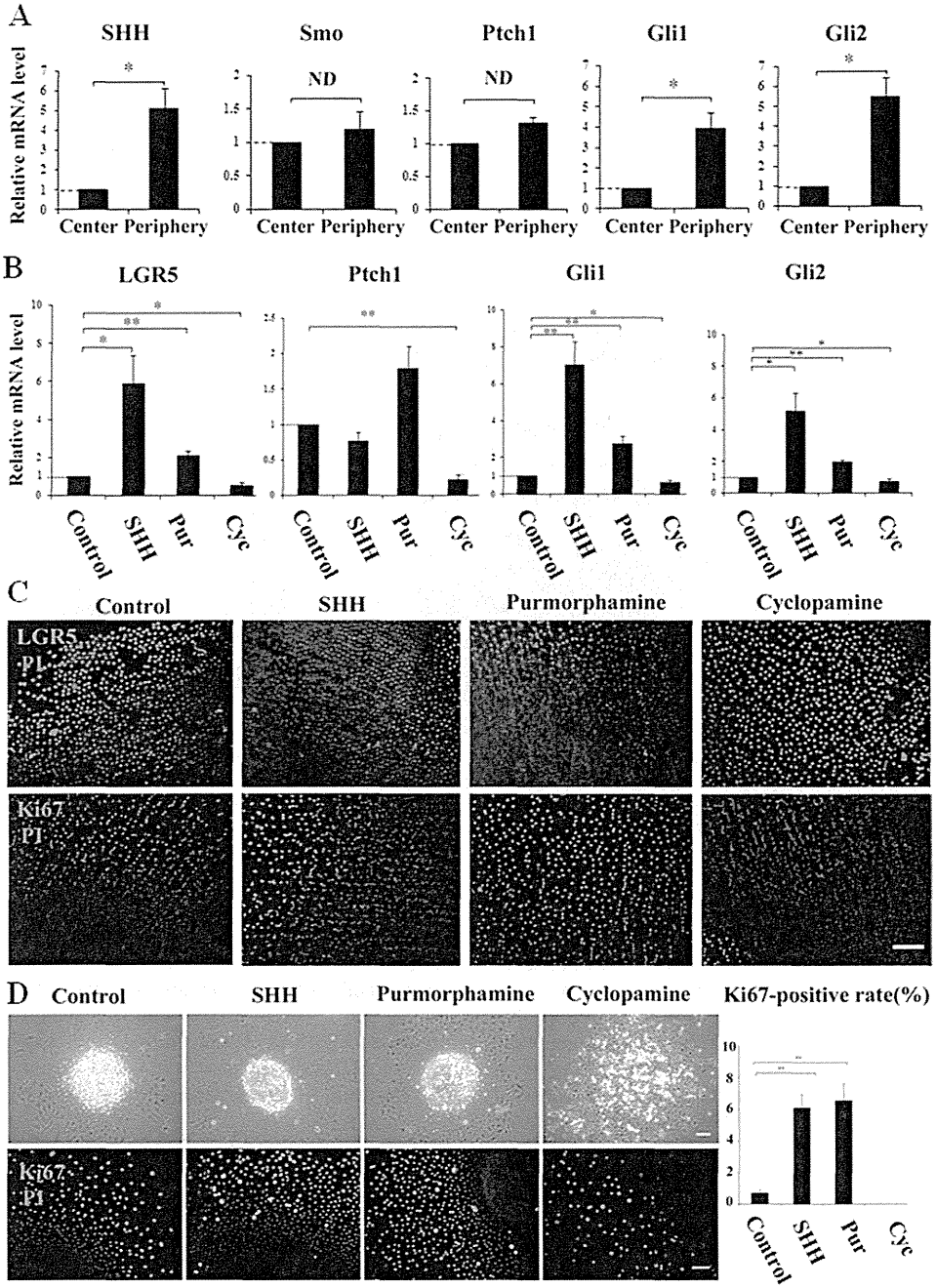

Figure 4. Hedgehog (HH) signaling pathway in corneal endothelial cells (CECs). **(A):** Real-time polymerase chain reaction (PCR) for HH signal-associated genes (*SHH*, *Smo*, *Ptch1*, *Gli1*, and *Gli2*) in central and peripheral human donor CECs. Mean ± SEM. *, $p < .05$. $n = 4$. **(B):** Real-time PCR of leucine-rich repeat G protein-coupled receptor 5 (*LGR5*), *Ptch1*, *Gli1*, and *Gli2* in human donor CECs treated with SHH, purmorphamine (Pur), and cyclopamine (Cyc), respectively. Mean ± SEM. *, $p < .05$; **, $p < .01$. $n = 4$. **(C):** Immunostaining of LGR5 and Ki67 in human donor CECs treated with SHH, Pur, and Cyc, respectively. Control: 0.1% dimethyl sulfoxide (DMSO). Scale bar = 100 μm. **(D):** Immunostaining of Ki67 in cultivated human CECs treated with SHH, Pur, and Cyc, respectively. Control: 0.01% DMSO. Scale bar = 100 μm. Ki67-positive rate of human CECs treated with SHH, Pur, and Cyc, respectively. Mean ± SEM. **, $p < .01$. $n = 5$. Abbreviations: LGR5, leucine-rich repeat G protein-coupled receptor 5; mRNA, messenger RNA; ND, No significant difference; PI, propidium iodide; SHH, sonic Hedgehog.

purmorphamine stimulation, whereas *LGR5* expression was reduced by cyclopamine stimulation at both the mRNA and protein levels (Fig. 4B, 4C). The expression patterns of *Gli1* and *Gli2* were similar to that of *LGR5*, but HH activation did not dramatically have an influence on *Ptch1*, the HH receptor (Fig. 4B).

Next, immunohistochemistry for Ki67 was performed to elucidate whether or not the HH pathway induced donor CEC proliferation. As human CECs are mitotically inactive and show weak-to-no proliferative capacity *in vivo* [3], an elevated expression of Ki67 was not observed in all experimental groups, suggesting that stimulation of the HH pathway alone is not sufficient to induce donor CEC proliferation (Fig. 4C). However, CECs reportedly retain the capacity to proliferate in vitro [4], so we investigated whether the HH pathway induced CEC proliferation in vitro. The expression of Ki67 was found

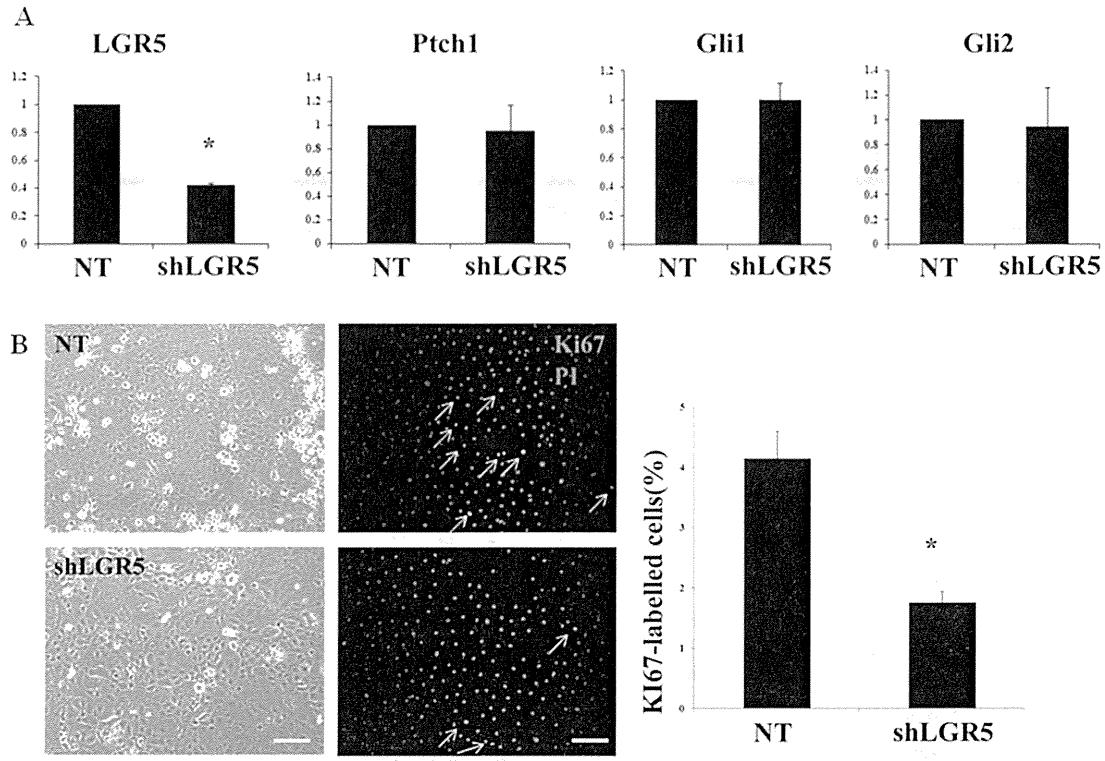

Figure 5. Effect of short hairpin *LGR5* (shLGR5) in human corneal endothelial cells (CECs). **(A):** Real-time polymerase chain reaction for leucine-rich repeat G protein-coupled receptor 5 (*LGR5*), *Ptch1*, *Gli1*, and *Gli2* in nontarget (NT)- and shLGR5-transfected cells. Mean ± SEM. *, $p < .05$. $n = 3$. **(B):** Phase contrast microscopy image and immunostaining of Ki67 in NT- and shLGR5-transfected human CECs. Arrows point to $Ki67^+$ cells. Scale bar = 100 μm. Mean ± SEM. *, $p < .05$. $n = 5$. Abbreviations: LGR5, leucine-rich repeat G protein-coupled receptor 5; NT, nontarget; PI, propidium iodide; shLGR5, short hairpin LGR5.

to be upregulated in response to SHH- and purmorphamine-stimulation, however, it was not upregulated in response to cyclopamine (Fig. 4D). These findings indicate that in the in vitro situation, the HH pathway is able to induce CEC proliferation. We posit that CECs treated with cyclopamine were unable to maintain their normal hexagonal morphology (Fig. 4D). Furthermore, Real-time PCR showed that the expression of *LGR5* in the cultured CECs with SHH stimulation was elevated as compared to those without SHH stimulation. Immunohistochemistry showed that after SHH stimulation, the expression of LGR5 in the cultured CECs was elevated in some of the cells, yet not in all of the cells (supplemental online Fig. 1). In view of these findings, we discovered for the first time that LGR5 is the target molecule of HH signaling in CECs and that CEC maintenance is partially regulated by the HH pathway.

Downregulation of LGR5 Decreased the Proliferation of CECs

The direct effect of LGR5 on the CECs was elucidated by the knockdown of *LGR5* by shRNA. For this experiment, primate cultivated CECs were used, due to the fact that cultured human CECs rarely express LGR5 (Fig. 2A, 2B). Nine sets of shRNA were designed, and the efficacy of their knockdown potential was then examined. Of those, shRNA-589 was found to be the most effective for knocking down the *LGR5* mRNA expression (approximately 60% knockdown) (Fig. 5A). Real-time PCR for *Ptch1, Gli1, and Gli2* showed that no significant differences were found between the short hairpin *LGR5* (shLGR5) group and the control (Fig. 5A). To demonstrate the effect of knocking down the *LGR5* gene on CEC proliferation, immunocytochemistry for Ki67 was performed. Compared with the control, cell morphology of the shLGR5-treated cells was not dramatically changed, however, the number of $Ki67^+$ cells in the shLGR5-treated cells was greatly reduced (Fig. 5B). These findings indicated that downregulation of *LGR5* did not have an effect on the HH pathway, but did decrease CEC proliferation in vitro.

Persistent *LGR5* Expression Inhibited MT Through the Wnt Pathway

To investigate the direct effects of persistent *LGR5* expression on CECs, we attempted to overexpress LGR5 using lentivirus containing CMV-*LGR5*- mRFP. In this experiment, human cultivated CECs (fourth passage, 62-year-old donor) were used, as they rarely express LGR5 (Fig. 2A). Real-time PCR showed that the expression of *LGR5* in *LGR5*-transfected cells (6 days after transfection) was about 60 times higher than that in NT vector-transfected cells ($p < .01$) (Fig. 6B). Immunofluorescence was used to confirm that the expression of *LGR5* in the LGR5-transfected cells was elevated in comparison with that in the NT cells (Fig. 6A). Of great interest, the relative mRNA levels of the HH signaling molecules in *LGR5*-transfected cells were downregulated as compared to those in the NT cells (Fig. 6B), indicating that LGR5 operates as a negative feedback regulator of the HH pathway.

Human CECs are reportedly vulnerable to morphological fibroblastic change under normal culture conditions [5]. To better demonstrate the effect of persistent *LGR5* expression, we used fourth-passaged cultivated CECs. After lentivirus transfection, some of the NT cells still exhibited an enlarged and elongated shape (fibroblastic change) (Fig. 6A). Of great

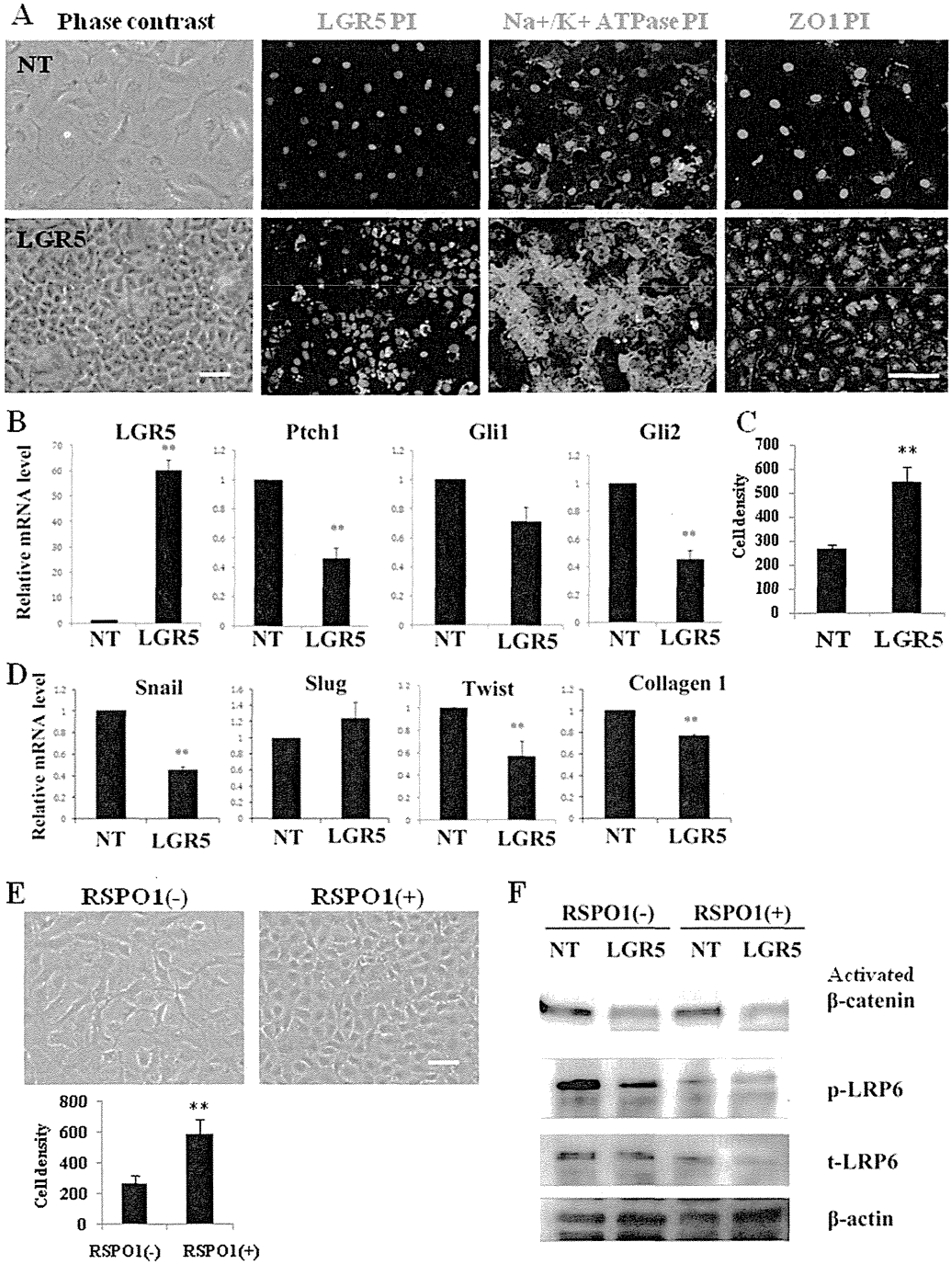

Figure 6. Function of leucine-rich repeat G protein-coupled receptor 5 (LGR5) and R-spondin-1 (RSPO1) in corneal endothelial cells (CECs). **(A):** Phase contrast microscopy image and immunostaining of LGR5, Na+/K+ ATPase, and ZO1 in nontarget (NT)- and *LGR5*-transfected human CECs. Scale bar = 100 μm. **(B):** Relative expression of *LGR5, Ptch1, Gli1, and Gli2* messenger RNA in NT- and *LGR5*-transfected cells. Mean ± SEM. **, $p < .01$. $n = 3$. **(C):** Cell density of NT- and *LGR5*-transfected cells. Mean ± SEM. **, $p < .01$. $n = 5$. **(D):** Real-time polymerase chain reaction for EMT-associated genes (*Snail, Slug, Twist, and collagen1*) in NT- and *LGR5*-transfected cells. Mean ± SEM. **, $p < .01$. $n = 3$. **(E):** Phase contrast image of human cultivated CECs with or without RSPO1 (50 ng/ml). Scale bar = 100 μm. Cell density of CECs with or without RSPO1. Mean ± SEM. **, $p < .01$. $n = 5$. **(F):** Western blotting of activated β-catenin, pLRP6, tLRP6, and β-actin in NT- and LGR5-transfected cells with or without RSPO1 (50 ng/ml). Abbreviations: LGR5, leucine-rich repeat G protein-coupled receptor 5; mRNA, messenger RNA; NT, nontarget; PI, propidium iodide; RSPO, R-spondin-1.

interest, the *LGR5*-transfected cells gradually changed their morphology and were shown to be compact, smaller-size, homogeneously hexagonal cells, resuming the normal physiological morphology (Fig. 6A). Cell density of the *LGR5*-transfected cells was found to be greatly elevated compared with that of the NT cells (Fig. 6C). To examine the function of cultivated CECs transfected with the NT and *LGR5* vector, immunohistochemistry was performed for Na^+/K^+ ATPase and ZO1. The expression of these two functional proteins was found to be much greater in the *LGR5*-transfected cells than in the NT cells, even though these expression patterns were not typical in comparison with those in in vivo CECs (Fig.

6A). In view of these findings, it is likely that LGR5 may be the key molecule for maintaining normal CEC phenotypes.

Transformation of endothelial cells to fibroblastic cells is known as endothelial–mesenchymal transformation (MT) [33]. The interesting findings observed in the *LGR5*-transfected cells led us to further study whether or not the persistent expression of *LGR5* was able to block the MT process. The expression level of epithelial-MT (EMT)-related molecules (*Snail, Slug, Twist, and Collagen1*) [34] was examined using real-time PCR. Of great importance, the relative mRNA level of all EMT markers except Slug were lower in the *LGR5*-transfected cells than in the NT cells (Fig. 6D), suggesting that persistent *LGR5* expression blocked the MT process. We further examined which pathway regulates the endothelial-MT observed in CECs. Recent studies suggest that the Wnt/β-catenin signaling pathway plays an important role in EMT [34]. Therefore, the expression level of Wnt/β-catenin-related molecules was examined using western blot analysis. Worthy of note, the protein level of cytosolic (non membrane bound) β-catenin and phosphorylated low-density-lipoprotein receptor-related protein 6 (p-LRP6) was greatly decreased in the LGR5-transfected cells (Fig. 6F). We found that the expression of β-catenin shifted from the cell membrane to the cytoplasm and nucleus, which is well observed in the typical EMT process, in most of nontarget transfected CECs. In contrast, we could observe the expression of β-catenin in cell membrane of LGR5-transfected CECs (supplemental online Fig. 2). These findings indicated that persistent LGR5 expression inhibited the corneal endothelial-MT through the Wnt/β-catenin pathway.

RSPO1-Accelerated CEC Proliferation and Inhibited MT Through the Wnt Pathway

Previously, LGR5 was thought to be an orphan receptor of the G protein-coupled receptor superfamily, and its ligand was unknown. However, several recent reports demonstrated that RSPOs function as ligands of LGR5 to regulate Wnt/β-catenin signaling [35–37]. Interestingly, we discovered that *RSPO1*, *2*, *3*, and *4* mRNA were expressed in the corneal epithelium, stroma, and endothelium, and that *RSPO1*, *2*, and *3* mRNA were only expressed in the peripheral-region CECs (supplemental online Fig. 3A). To determine the function of RSPOs on CEC differentiation, we cultured the primary human CECs with or without human recombinant RSPOs. Worthy of note, 7 days after culture, only cultivated human CECs treated with RSPO1 [50 ng/ml] showed the compact, smaller-size, homogeneously hexagonal cells, whereas other RSPOs did not have an obvious effect on CEC differentiation in vitro (supplemental online Fig. 3B). To determine the function of RSPOs on donor CEC proliferation, we performed immunohistochemistry for Ki67. Most surprisingly and very interestingly, human donor CECs incubated with RSPO1 (50 ng/ml) for 48 hours at 37°C showed a dramatically increased level of $Ki67^+$ cell ratios as compared to other RSPOs (supplemental online Fig. 3C). In view of these findings, we think that among the RSPOs family, RSPO1 in particular may play an important role in the maintenance of CECs.

Finally, to further determine the effect of RSPO1 on CECs, we maintained the secondary culture of human CECs with or without RSPO1. Through culturing the CECs in both conditions, we clearly observed that the cultured cells with RSPO1 maintained their hexagonal morphology, whereas some of the cultured cells without RSPO1 still showed fibroblastic phenotypes (Fig. 6E). Moreover, the cell density of RSPO1-treated cells was elevated in comparison with that of the nontreated cells (Fig. 6E). To demonstrate which pathway regulates this type of corneal endothelial MT, we examined the expression level of Wnt/β-catenin-related molecules using western blot analysis. We performed the experiments twice, and the results were nearly identical; the protein level of cytosolic β-catenin and p-LRP6 in the LGR5-transfected cells treated with RSPO1 was decreased in comparison with that in the NT cells (Fig. 6F). Moreover, the protein levels of the RSPO1-treated NT and LGR5-transfected cells were more decreased as compared to the cells not treated with RSPO1 (Fig. 6F). These results suggested that the stimulation of cells overexpressing LGR5 with RSPO1 accelerates pLRP degradation and β-catenin turnover.

Discussion

Cornea tissue is extremely important, as most mammals acquire the majority of their external information through it. Recently, particular attention has been focused on CECs due to the fact that the corneal transplantation procedure is currently undergoing a paradigm shift from keratoplasty to endothelial keratoplasty. Therefore, both scientifically and clinically, to establish the next generation of novel therapy for treating cornea-related blindness worldwide, it is extremely important to understand the molecular mechanism of corneal endothelial stem/progenitor cells. However, very little is presently known about those molecular mechanisms.

It has been reported that the characteristics and proliferative potential of CECs are different between those located at the central region of the cornea and those located at the peripheral region of the cornea [38, 39], and a study has shown that the cornea has a higher density of endothelial cells in the peripheral region than in the central region [40]. Moreover, CECs from the peripheral region reportedly retain higher replication ability than those from the central region [12], and peripheral-region CECs contain more precursors and have a stronger self-renewal capacity than CECs in the central region [41]. He et al. recently identified a novel anatomic organization in the peripheral region of human corneal endothelium, suggesting a continuous slow centripetal migration of CECs from specific niches [15]. Thus, it is most likely that human corneal endothelial stem/progenitor cells are mainly distributed in the peripheral region. In fact, no stem/progenitor cell marker for CECs has thus-far been elucidated, and the results of this study demonstrate for the first time that CECs exhibit regional diversity with respect to LGR5 expression. In view of these findings and the unique expression pattern of LGR5 in CECs, LGR5 might represent a first marker for corneal endothelial stem-cell-containing populations.

It has been reported that cell size may distinguish keratinocyte stem cells from transient amplifying cells or differentiated cells [28]. In the epidermis, the response to phorbol esters of the smallest keratinocytes is different from that of other cells. Those keratinocytes also exhibited the highest clonogenicity. Even though CECs are different from ectoderm-derived keratinocytes, the average diameter of the $LGR5^+$ cells in this study was in fact smaller than that of the $LGR5^-$ cells. Based on these findings, and on the findings of the above-cited previous report regarding the size of peripheral CECs, it is possible that cell size might be a potential indicator of corneal endothelial stem/progenitor cells.

We found that LGR5 is a key molecule for maintaining the integrity of CECs and regulating normal cell phenotypes in vitro. We also found that isolated cells fractionated based on the intensity of their LGR5 expression could produce different cell populations with different properties. Only cells in

the LGR5$^+$ population exhibited exceptionally high proliferative potential, features associated with stem/progenitor cell populations. Based on these findings, the unique expression pattern and necessity in the in vitro condition, there is possibly a link between LGR5 and the function of corneal endothelial stem/progenitor cells.

Previous studies have indicated that high concentration of SHH caused a marked increase in retinal progenitor cell proliferation and a general increase in the accumulation of differentiated cells [29]. The findings of this present manuscript show that in the in vitro situation, the HH pathway is able to induce CEC proliferation, consistent with the findings of previous reports. HH is a family of secreted molecules that serve as morphogens during multiple aspects of development in a wide range of tissue types. HH is involved in the left-right asymmetry decision and anterior–posterior axis decision in limb pattern determination by regulating cell proliferation and survival. In CECs, there is regional variation of HH signal activity, and based on our findings, HH signaling might possibly control corneal endothelial morphogenesis.

RSPOs are a family of four cysteine-rich secreted proteins that were isolated as strong potentiators of Wnt/β-catenin signaling. A vast amount of information regarding the cell biological functions of RSPOs has emerged over the last several years, especially with respect to their role as ligands of the orphan receptors LGR 4/5/6. These updated and important findings led us to further study whether RSPOs may have an effect on the function of human CECs. As human CECs are mitotically inactive and are essentially nonregenerative in vivo, corneal endothelial loss due to disease or trauma is followed by a compensatory enlargement of the remaining endothelial cells. To the best of our knowledge, there are no reports regarding a useful inductive reagent or molecule to increase the level of human CEC proliferation and CEC density, although we previously developed the CECs culture protocol using Y-27632 [21, 22]. We examined the expression of RSPO1 in CECs and found that its protein level is quite low (data no shown), suggesting that external RSPO1, rather than internal RSPO1, plays a critical role in maintaining the CEC function. Moreover, although there was no expression of LGR5 in the cultured CECs, RSPO1 did have some effect on the condition of CECs in vitro. We do not precisely know the reason why, but from our results, we presume that the effect of RSPO1 on CECs might be of both an LGR5-dependent and -independent manner. The findings of this study show for the first time that CECs incubated with RSPO1 exhibited a dramatically increased level of cell proliferation and cell density, suggesting that it might represent a first candidate molecule for reconstructing the damaged cornea through topical application or for use as a culture reagent.

Several studies suggest that the Wnt/β-catenin pathway plays an important role in EMT and that activation of Wnt/β-catenin-dependent signaling modulates the expression of EMT-related genes [34]. However, previous reports have indicated that RSPOs potentiate Wnt/β-catenin signaling by actually functioning as a ligand of LGR5 [35–37]. The exact mechanism involved in this activation is still unclear and there are several conflicting findings as to whether LGR5 is a positive or negative regulator of the Wnt pathway [42–44]. One possible explanation is that the molecular mechanism depends on the tissues, organs, and the species of animal. The cornea is a unique avascular tissue, and its health is maintained by tears and aqueous humor. In contrast, the health of most other organs is maintained by vascular support, suggesting that the characteristics and mechanism of corneal cells are fundamentally different from the epithelial cells of other tissues. Thus, based on the findings of this study, RSPO1 dramatically accelerates CEC proliferation and inhibits corneal endothelial MT through the Wnt pathway.

Conclusion

In conclusion, the findings of this study are the first to demonstrate the function of LGR5 in human CECs (supplemental online Fig. 4). LGR5 has proven to be a powerful tool in identifying a multitude of stem/progenitor cell populations. Through the regulation of LGR5 through the HH and Wnt pathways, CEC integrity was well structured and maintained. In addition, the LGR5 ligand RSPO1 may exploit the novel substantial protocol to provide the efficient expansion of CECs, suggesting that RSPO1-based three dimensional culture and medical treatments hold promise for regenerative therapy, not only for the treatment of corneal dysfunctions, but also for a variety of severe general diseases.

Acknowledgments

The authors wish to thank Yuiko Hata, Rie Yasuda, Kenta Yamazaki, Yuji Sakamoto, and Shoki Okura for assisting with the experimental procedures, and John Bush for reviewing the manuscript. Drs. Noriko Koizumi and Shigeru Kinoshita had applied for the patent regarding the use of ROCK inhibitor on corneal endothelial research (WO/2009/028631). This study was supported in part by Grants-in-Aid for scientific research from the Highway Program for realization of regenerative medicine, the JST-ETH Strategic Japanese-Swiss Cooperative Program and OptiStem.

Disclosure of Potential Conflicts of Interest

The authors indicate no potential conflicts of interest.

References

1 Whitcher JP, Srinivasan M, Upadhyay MP. Corneal blindness: a global perspective. Bull World Health Organ 2001;79:214–221.
2 Tan DT, Dart JK, Holland EJ et al. Corneal transplantation. Lancet 2012;379:1749–1761.
3 Joyce NC. Proliferative capacity of the corneal endothelium. Prog Retin Eye Res 2003;22:359–389.
4 Engelmann K, Bohnke M, Friedl P. Isolation and long-term cultivation of human corneal endothelial cells. Invest Ophthalmol Vis Sci 1988; 29:1656–1662.
5 Peh GS, Beuerman RW, Colman A et al. Human corneal endothelial cell expansion for corneal endothelium transplantation: an overview. Transplantation 2011;91:811–819.
6 Blanpain C, Horsley V, Fuchs E. Epithelial stem cells: turning over new leaves. Cell 2007;128:445–458.
7 De Luca M, Pellegrini G, Green H. Regeneration of squamous epithelia from stem cells of cultured grafts. Regen Med 2006;1:45–57.
8 Lavker RM, Sun TT. Epithelial stem cells: the eye provides a vision. Eye (Lond) 2003;17:937–942.
9 Cotsarelis G, Cheng SZ, Dong G et al. Existence of slow-cycling limbal epithelial basal cells that can be preferentially stimulated to proliferate: implications on epithelial stem cells. Cell 1989;57: 201–209.

10 Pellegrini G, Golisano O, Paterna P et al. Location and clonal analysis of stem cells and their differentiated progeny in the human ocular surface. J Cell Biol 1999;145:769–782.
11 Schermer A, Galvin S, Sun TT. Differentiation-related expression of a major 64K corneal keratin in vivo and in culture suggests limbal location of corneal epithelial stem cells. J Cell Biol 1986;103: 49–62.
12 Mimura T, Joyce NC. Replication competence and senescence in central and peripheral human corneal endothelium. Invest Ophthalmol Vis Sci 2006;47:1387–1396.
13 Whikehart DR, Parikh CH, Vaughn AV et al. Evidence suggesting the existence of stem cells for the human corneal endothelium. Mol Vis 2005;11:816–824.
14 McGowan SL, Edelhauser HF, Pfister RR et al. Stem cell markers in the human posterior limbus and corneal endothelium of unwounded and wounded corneas. Mol Vis 2007;13:1984–2000.
15 He Z, Campolmi N, Gain P et al. Revisited microanatomy of the corneal endothelial periphery: new evidence for continuous centripetal migration of endothelial cells in humans. Stem Cells 2012;30: 2523–2534.
16 Barker N, van Es JH, Kuipers J et al. Identification of stem cells in small intestine and colon by marker gene Lgr5. Nature 2007;449: 1003–1007.
17 Jaks V, Barker N, Kasper M et al. Lgr5 marks cycling, yet long-lived, hair follicle stem cells. Nat Genet 2008;40:1291–1299.
18 Barker N, Huch M, Kujala P et al. Lgr5(+ve) stem cells drive self-renewal in the stomach and build long-lived gastric units in vitro. Cell Stem Cell 2010;6:25–36.
19 Tanese K, Fukuma M, Yamada T et al. G-protein-coupled receptor GPR49 is up-regulated in basal cell carcinoma and promotes cell proliferation and tumor formation. Am J Pathol 2008;173:835–843.
20 Koizumi N, Okumura N, Kinoshita S. Development of new therapeutic modalities for corneal endothelial disease focused on the proliferation of corneal endothelial cells using animal models. Exp Eye Res 2012;95:60–67.
21 Koizumi N, Sakamoto Y, Okumura N et al. Cultivated corneal endothelial cell sheet transplantation in a primate model. Invest Ophthalmol Vis Sci 2007;48:4519–4526.
22 Okumura N, Koizumi N, Ueno M et al. ROCK inhibitor converts corneal endothelial cells into a phenotype capable of regenerating in vivo endothelial tissue. Am J Pathol 2012;181:268–277.
23 Nakamura T, Endo K, Kinoshita S. Identification of human oral keratinocyte stem/progenitor cells by neurotrophin receptor p75 and the role of neurotrophin/p75 signaling. Stem Cells 2007;25:628–638.
24 Nakamura T, Ohtsuka T, Sekiyama E et al. Hes1 regulates corneal development and the function of corneal epithelial stem/progenitor cells. Stem Cells 2008;26:1265–1274.
25 Nakatsukasa M, Kawasaki S, Yamasaki K et al. Tumor-associated calcium signal transducer 2 is required for the proper subcellular localization of claudin 1 and 7: implications in the pathogenesis of gelatinous drop-like corneal dystrophy. Am J Pathol 2010;177: 1344–1355.
26 Aghib DF, McCrea PD. The E-cadherin complex contains the src substrate p120. Exp Cell Res 1995;218:359–369.
27 Van Horn DL, Hyndiuk RA. Endothelial wound repair in primate cornea. Exp Eye Res 1975;21:113–124.
28 Barrandon Y, Green H. Cell size as a determinant of the clone-forming ability of human keratinocytes. Proc Natl Acad Sci U S A 1985;82:5390–5394.
29 Stanton BZ, Peng LF. Small-molecule modulators of the Sonic Hedgehog signaling pathway. Mol Biosyst 2010;6:44–54.
30 Tsuru T, Araie M, Matsubara M et al. Endothelial wound-healing of monkey cornea: fluorophotometric and specular microscopic studies. Jpn J Ophthalmol 1984;28:105–125.
31 Sinha S, Chen JK. Purmorphamine activates the Hedgehog pathway by targeting Smoothened. Nat Chem Biol 2006;2:29–30.
32 Chen JK, Taipale J, Cooper MK et al. Inhibition of Hedgehog signaling by direct binding of cyclopamine to Smoothened. Genes Dev 2002;16:2743–2748.
33 Lee HT, Lee JG, Na M et al. FGF-2 induced by interleukin-1 beta through the action of phosphatidylinositol 3-kinase mediates endothelial mesenchymal transformation in corneal endothelial cells. J Biol Chem 2004;279:32325–32332.
34 Lee JM, Dedhar S, Kalluri R et al. The epithelial-mesenchymal transition: new insights in signaling, development, and disease. J Cell Biol 2006;172:973–981.
35 Carmon KS, Gong X, Lin Q et al. R-spondins function as ligands of the orphan receptors LGR4 and LGR5 to regulate Wnt/beta-catenin signaling. Proc Natl Acad Sci U S A 2011;108:11452–11457.
36 de Lau W, Barker N, Low TY et al. Lgr5 homologues associate with Wnt receptors and mediate R-spondin signalling. Nature 2011;476: 293–297.
37 Glinka A, Dolde C, Kirsch N et al. LGR4 and LGR5 are R-spondin receptors mediating Wnt/beta-catenin and Wnt/PCP signalling. EMBO Rep 2011;12:1055–1061.
38 Bednarz J, Rodokanaki-von Schrenck A, Engelmann K. Different characteristics of endothelial cells from central and peripheral human cornea in primary culture and after subculture. In Vitro Cell Dev Biol Anim 1998;34:149–153.
39 Patel SP, Bourne WM. Corneal endothelial cell proliferation: a function of cell density. Invest Ophthalmol Vis Sci 2009;50:2742–2746.
40 Schimmelpfennig BH. Direct and indirect determination of nonuniform cell density distribution in human corneal endothelium. Invest Ophthalmol Vis Sci 1984;25:223–229.
41 Mimura T, Yamagami S, Yokoo S et al. Comparison of rabbit corneal endothelial cell precursors in the central and peripheral cornea. Invest Ophthalmol Vis Sci 2005;46:3645–3648.
42 Garcia MI, Ghiani M, Lefort A et al. LGR5 deficiency deregulates Wnt signaling and leads to precocious Paneth cell differentiation in the fetal intestine. Dev Biol 2009;331:58–67.
43 Schuijers J, Clevers H. Adult mammalian stem cells: the role of Wnt, Lgr5 and R-spondins. EMBO J. 2012.
44 Walker F, Zhang HH, Odorizzi A et al. LGR5 is a negative regulator of tumourigenicity, antagonizes Wnt signalling and regulates cell adhesion in colorectal cancer cell lines. Plos One 2011;6:e22733.

See www.StemCells.com for supporting information available online.

A Randomized, Multicenter Phase 3 Study Comparing 2% Rebamipide (OPC-12759) with 0.1% Sodium Hyaluronate in the Treatment of Dry Eye

*Shigeru Kinoshita, MD, PhD,[1] Kazuhide Oshiden, MS,[2] Saki Awamura, BS,[2] Hiroyuki Suzuki, BS,[2] Norihiro Nakamichi, MS,[2] Norihiko Yokoi, MD, PhD,[1] for the Rebamipide Ophthalmic Suspension Phase 3 Study Group**

Objective: To investigate the efficacy of 2% rebamipide ophthalmic suspension compared with 0.1% sodium hyaluronate ophthalmic solution for the treatment of patients with dry eye.

Design: Randomized, multicenter, active-controlled parallel-group study.

Participants: One hundred eighty-eight patients with dry eye.

Methods: Following a 2-week screening period, patients were allocated randomly to receive 2% rebamipide or 0.1% sodium hyaluronate, administered as 1 drop in each eye 4 or 6 times daily, respectively, for 4 weeks.

Main Outcome Measures: There were 2 primary end points: changes in the fluorescein corneal staining (FCS) score to determine noninferiority of 2% rebamipide and changes in the lissamine green conjunctival staining (LGCS) score to determine superiority. Secondary objective end points were Schirmer's test results and tear film breakup time (TBUT). Secondary subjective end points were dry eye–related ocular symptoms (foreign body sensation, dryness, photophobia, eye pain, and blurred vision) score and the patients' overall treatment impression score.

Results: In the primary analysis, the mean change from baseline in FCS scores verified noninferiority, indicated significant improvement, and, in LGCS scores, verified the superiority of 2% rebamipide to 0.1% sodium hyaluronate. Values for the Schirmer's test and TBUT were comparable between the 2 groups. For 2 dry eye–related ocular symptoms—foreign body sensation and eye pain—2% rebamipide showed significant improvements over 0.1% sodium hyaluronate. Patients had a significantly more favorable impression of 2% rebamipide than of 0.1% sodium hyaluronate; 64.5% rated treatment as improved or markedly improved versus 34.7%, respectively. No serious adverse events were observed.

Conclusions: Administration of 2% rebamipide was effective in improving both the objective signs and subjective symptoms of dry eye. Those findings, in addition to the well-tolerated profile of 2% rebamipide, clearly show that it is an effective therapeutic method for dry eye.

Financial Disclosure(s): Proprietary or commercial disclosure may be found after the references.

Ophthalmology 2013;120:1158–1165 © 2013 by the American Academy of Ophthalmology.

**Group members listed online (available at http://aaojournal.org).*

Dry eye is a multifactorial disease of the tears and ocular surface that results in symptoms of discomfort, visual disturbance, and tear film instability with potential damage to the ocular surface.[1] Dry eye is one of the most common ophthalmologic problems,[2] and it is estimated that up to one-third of the population worldwide may be affected.[2–4] The effect on quality of life is substantial because of symptoms such as pain and irritation, which have a negative effect on ocular health, general health, and well-being and often disrupt daily activities.[2,5] Dry eye is caused by disease or disruption to components of the ocular surface[1,6] that help to maintain its integrity, driven by tear hyperosmolarity and tear film instability.[1] The tear film can be destabilized by decreased tear production or altered tear composition, damaging the ocular surface and resulting in inflammation and, ultimately, further tear film instability.[1]

Currently, tear supplementation with artificial tears is considered a mainstay treatment for cases of mild-to-moderate dry eye; however, frequent instillation often is required.[5] Sodium hyaluronate has shown some effectiveness in patients with dry eye.[7–9] Insertion of punctal plugs or permanent punctal occlusion also are options for cases of moderate or severe dry eye,[10] although a reduction in symptom relief over time has been reported.[11] Thus, treatment options are limited, especially for moderate-to-severe dry eye.

Recently, the role of ocular mucins has been attracting increased attention for the treatment of dry eye. The tear

ISSN 0161-6420/13/$–see front matter
http://dx.doi.org/10.1016/j.ophtha.2012.12.022

film currently is understood as being a meta-stable aqueous gel with a mucin gradient that decreases from the ocular surface to the undersurface of the outermost lipid layer.[12] Mucins are of 2 types, 1 type being secreted by goblet cells and the other type being expressed on the membranes of ocular surface epithelia.[6,13] In dry eye, reduced goblet cell density[14] and changes in mucin amount, distribution, and glycosylation have been reported,[15,16] and therapeutic improvements reportedly have occurred when mucin instillation is administered in patients with dry eye.[17]

Rebamipide (OPC-12759; Otsuka Pharmaceutical Co, Ltd, Tokyo, Japan) is a quinolinone derivative with mucin secretagogue activity,[18–20] and in Japan, rebamipide is marketed as an oral therapeutic drug of gastric mucosal disorders and gastritis under the trade name Mucosta in 2 forms: 100-mg tablets and 20% granules. When rebamipide was instilled in rabbit eyes, rebamipide increased the production of mucin-like substances and the number of periodic acid–Schiff-positive cells.[21,22] A recent study also reported a significant increase in a mucin-like glycoprotein and *MUC1* and *MUC4* gene expression after human corneal epithelial cells were incubated with rebamipide.[23] A phase 2 study in patients with dry eye showed that a 4-week treatment with 2% rebamipide ophthalmic suspension was significantly more effective than the placebo in terms of improving the fluorescein corneal staining (FCS) score, the lissamine green conjunctival staining (LGCS) score, and tear film breakup time (TBUT), as well as subjective symptoms (foreign body sensation, dryness, photophobia, eye pain, and blurred vision) and the patients' overall treatment impression.[24]

The objective of this study was to compare the efficacy of 2% rebamipide ophthalmic suspension with that of 0.1% sodium hyaluronate ophthalmic solution in patients with dry eye in terms of noninferiority in FCS score and superiority in LGCS score. This was a phase 3 trial designed to confirm the efficacy of 2% rebamipide for registration purposes. Sodium hyaluronate was selected as the active control because it is an indicated treatment for keratoconjunctival disorder accompanying dry eye in Japan and has demonstrated clinical efficacy.[7–9]

Materials and Methods

Study Design

This was a randomized, multicenter, active-controlled, parallel-group phase 3 trial conducted in 3 phases: screening, evaluation, and follow-up. As much as possible, the study was conducted under masked conditions for the investigators; the perfect masked conditions could not be accomplished because the instillation frequency and chemical properties differ between the rebamipide ophthalmic suspension and the sodium hyaluronate ophthalmic solution. During the initial 2-week screening period, the patients received preservative-free artificial tears (Soft Santear; Santen Pharmaceutical Co, Ltd, Osaka, Japan) 4 times daily, 1 drop per application. This screening period was performed to minimize the effects of any eye drops used before screening.

Eligible patients were allocated randomly to receive 2% rebamipide or 0.1% sodium hyaluronate. Central randomization was adopted for assigning patients to each group in a 1:1 ratio by using a dynamic allocation[25] of stratified centers, with or without Sjögren's syndrome and baseline FCS scores (4–6, 7–9, and 10–15).

Patients in the rebamipide group received 2% rebamipide ophthalmic suspension, 1 drop in each eye 4 times daily. Patients in the sodium hyaluronate group received 0.1% sodium hyaluronate ophthalmic solution (Hyalein Mini ophthalmic solution 0.1%; Santen Pharmaceutical Co, Ltd) 1 drop in each eye 6 times daily. For both groups, the total treatment period was 4 weeks, and examinations were conducted at week 2 and week 4 after the start of treatment. To monitor safety, follow-up examinations were conducted 2 weeks after the end of treatment.

The study was conducted in accordance with the ethical principles set forth in the Declaration of Helsinki and the Good Clinical Practice Guidelines. The study protocol and informed consent were reviewed and approved by the institutional review board before initiation. Written informed consent was obtained from each patient before the start of the study. The study was registered before patient enrollment (clinical trial identifier NCT00885079; accessed July 26, 2012).

Patients

Eligible patients were 20 years of age or older and had dry eye–related symptoms that were not fully relieved by conventional treatments (e.g., artificial tears), with symptoms present for more than 20 months before the screening examination. Other inclusion criteria were: (1) score of 2 or more for 1 or more dry eye–related ocular symptom(s), (2) an FCS score of 4 or more, (3) an LGCS score of 5 or more, (4) a no-anesthesia Schirmer's test value at 5 minutes of 5 mm or less, and (5) best-corrected visual acuity of 20/100 or better. These criteria needed to be met at both the screening and baseline examinations, with criteria 2 through 4 being met in the same eye.

Exclusion criteria included (1) anterior ocular disease (such as blepharitis or blepharospasm), (2) continued use of eye drops, (3) patients who had a punctal plug or had it removed within 3 months before the screening examination, and (4) patients who underwent an operation to the ocular surface within 12 months or intraocular surgery within 3 months before the screening period.

The following drugs or therapies were prohibited from the screening examination to the end of study treatment: rebamipide for gastric mucosal disorders and gastritis; any prescription or over-the-counter ophthalmic drugs (except Soft Santear during the screening period); contact lenses; and ocular surgery or any other treatment affecting the dynamics of tear fluid, including its nasolacrimal drainage process. The inclusion criteria, exclusion criteria, and prohibited drugs or therapies used in this study have been described previously[24] and were the same as those used for a phase 2 study.

Assessment of Outcome Measures

Efficacy Assessments. Efficacy was evaluated primarily with an objective measure and secondarily with objective and subjective measures. There were 2 primary objective end points, FCS and LGCS scores. Secondary objective end points were TBUT and the Schirmer's test value. Secondary subjective end points included dry eye–related ocular symptoms (foreign body sensation, dryness, photophobia, eye pain, and blurred vision) and the patient's overall treatment impression. All of these parameters were assessed at baseline, at week 2, at week 4, or at treatment discontinuation, except for the Schirmer's test assessed at baseline, at week 4, or at treatment discontinuation, and the patient's overall treatment impression was assessed at week 4 or at treatment discontinuation.

For FCS, 5 μl 2% fluorescein solution (provided by the sponsor) was instilled in the conjunctival sac as the patient blinked normally. Corneal staining was examined under standard illumination using a slit-lamp microscope with a cobalt blue filter. According to the National Eye Institute/Industry Workshop report, the cornea was divided into 5 fractions,[26] each fraction given a staining score from 0 through 3, and the total score then was calculated. The sponsor provided each investigator with a set of photographs of FCS and LGCS to ensure standardization when scoring.

For LGCS, 20 μl 1% lissamine green solution (provided by the sponsor) was instilled in the conjunctival sac, and the conjunctiva was divided into 6 fractions.[26] Conjunctival staining was evaluated under low illumination by slit-lamp microscopy and was scored from 0 through 3 for each fraction, then summed to calculate the total score.

For TBUT, 5 μl 2% fluorescein solution was instilled in the conjunctival sac, and TBUT was then evaluated by slit-lamp microscopy. The elapsed time from a normal blink to the first appearance of a dry spot in the tear film was measured 3 times.

The Schirmer's test was performed without anesthesia to measure tear volume as follows. A Schirmer's test strip was placed on the lower eyelid between eyelid conjunctiva and bulbar conjunctiva without touching the cornea. The tear volume then was measured for 5 minutes after the patient was instructed to close the eyelid lightly. The length in millimeters of tear fluid absorbed on the strip measured from the edge of the strip was recorded as tear volume.

Dry eye–related ocular symptoms, such as foreign body sensation, dryness, photophobia, eye pain, and blurred vision were examined by questioning each patient. These symptoms were scored from 0 through 4; a score of 0 indicated no symptoms and a score of 4 indicated very severe symptoms.

The patient's overall treatment impression was examined by questioning each patient and was scored from 1 through 7, a score of 1 being markedly improved compared with baseline and a score of 7 being markedly worsened compared with baseline.

Safety Assessments. The safety variable was the occurrence of adverse events, determined at various visits by means of physical signs and symptoms, external eye examination and slit-lamp microscopy, visual acuity, intraocular pressure, funduscopy, and clinical laboratory tests including hematology, biochemistry, and urinalysis.

Statistical Analyses

Sample size calculation was performed based on data from the previous trial.[24] Using the FCS score, by assuming the mean difference between the 2% rebamipide group and the 0.1% sodium hyaluronate group to be 0.7, with a standard deviation of 2.3, a significance level of 5%, and the noninferiority margin to be 0.4, the number of patients to verify noninferiority was calculated. The results showed that the power exceeded 80% when 85 patients were included per group. In addition, using the LGCS score, by assuming the mean difference between the 2% rebamipide group and the 0.1% sodium hyaluronate group to be 1.4, with a standard deviation of 3.1, and a significance level of 5%, the number of patients required to verify superiority was calculated. The results showed that the power exceeded 80% when 80 patients were included per group. On the basis of above results, the number of patients was set at 90 per group to allow for those who might be excluded from the efficacy analysis. Missing efficacy data, including those resulting from early study termination, were corrected by the last observation carried forward (LOCF) method. In the analysis of dry eye–related ocular symptoms, patients with a dry eye–related ocular symptom score of 0 at baseline were excluded. Missing safety data were treated as missing.

All patients who were enrolled in the study were included in the efficacy and safety analyses. A closed test procedure was used for multiplicity considerations of 2 primary end points. First, noninferiority was assessed in FCS. If the noninferiority was confirmed, the superiority was examined in LGCS. Noninferiority for change from baseline in the FCS score (LOCF) was determined by comparing the noninferiority margin (0.4) with the upper limit of the 95% confidence interval of the difference between the 2 treatment groups. Superiority was verified by comparing t test results for change from baseline in the LGCS score (LOCF) between the 2 treatment groups. Furthermore, an analysis of change from baseline of FCS and LGCS score at each visit and secondary end points was performed using the t test or Wilcoxon signed-rank test. The level of significance was 5% (2-sided).

The eye in which objective efficacy end points were analyzed was determined as follows: (1) if only 1 eye met the inclusion criteria, then this eye was used; (2) if both eyes met the inclusion criteria, the eye with the higher FCS baseline score was used; (3) if both eyes had the same FCS baseline score, then the eye with the higher LGCS baseline score was used; and (4) if both eyes had the same LGCS baseline score, the right eye was used.

Results

Participant Characteristics

A total of 188 patients were allocated randomly to receive 1 of the 2 treatments: 93 patients entered the 2% rebamipide group and 95 patients entered the 0.1% sodium hyaluronate group. In total, 96.8% of the patients completed the trial (Table 1). Patient characteristics across the treatment groups were comparable (Table 2). Of the total 188 participants, 163 were female (86.7%) and the mean age ± standard deviation was 56.6±17.4 years. Of the 188 patients, 34 patients (18.1%) had primary or secondary Sjögren's syndrome as the underlying cause of dry eye.

Table 1. Patient Disposition

	Total	2% Rebamipide	0.1% Sodium Hyaluronate
Randomized and treated	188	93	95
Completed	182 (96.8)	91 (97.8)	91 (95.8)
Discontinued	6 (3.2)	2 (2.2)	4 (4.2)
Occurrence of adverse events	4 (2.1)	1 (1.1)	3 (3.2)
Patient's wish	2 (1.1)	1 (1.1)	1 (1.1)

Data are presented as number (%).

Table 2. Demographics and Other Baseline Characteristics

	2% Rebamipide (n = 93)	0.1% Sodium Hyaluronate (n = 95)	*P* Value*
Gender			
Male	10 (10.8)	15 (15.8)	0.309
Female	83 (89.2)	80 (84.2)	
Age (yrs)			
20–49	29 (31.2)	35 (36.8)	0.713
50–64	26 (28.0)	24 (25.3)	
≥65	38 (40.9)	36 (37.9)	
Main cause or primary disease of dry eye			
Primary Sjögren's syndrome	11 (11.8)	9 (9.5)	0.766
Secondary Sjögren's syndrome	6 (6.5)	8 (8.4)	
Other systemic disease	0 (0)	0 (0)	
Ocular disease	0 (0)	0 (0)	
Menopause	1 (1.1)	0 (0)	
Unknown	75 (80.6)	78 (82.1)	
Fluorescein corneal staining score†			
4–6	47 (50.5)	47 (49.5)	0.985
7–9	32 (34.4)	33 (34.7)	
10–15	14 (15.1)	15 (15.8)	
Dry eye–related ocular symptom†			
Foreign body sensation	69 (74.2)	68 (71.6)	0.686
Dryness	76 (81.7)	87 (91.6)	0.046
Photophobia	62 (66.7)	53 (55.8)	0.126
Eye pain	50 (53.8)	58 (61.1)	0.312
Blurred vision	53 (57.0)	55 (57.9)	0.900

Data are presented as number (%) unless otherwise indicated.
*Chi-square test (Fisher exact test in the case of presence of cell with a frequency of lower than 5).
†At baseline.

Efficacy Evaluation

Primary End Points. At baseline, the mean FCS scores were 7.0 in both groups. The mean change from baseline to LOCF in FCS score was −3.7 for the 2% rebamipide group and −2.9 for the 0.1% sodium hyaluronate group (Fig 1A and Table 3). The 95% confidence interval of the difference between the 2 treatment groups was −1.47 to −0.24, and the upper limit was lower than the noninferiority margin of 0.4. Therefore, the noninferiority of 2% rebamipide to 0.1% sodium hyaluronate was verified. In addition, the 95% confidence interval did not include 0, indicating the significant improvement of 2% rebamipide to 0.1% sodium hyaluronate. At baseline, mean LGCS scores were similar between groups (9.8 for 2% rebamipide vs. 10.1 for 0.1% sodium hyaluronate). The mean change from baseline to LOCF in LGCS score was −4.5 for the 2% rebamipide group and −2.4 for the 0.1% sodium hyaluronate group (Fig 1B and Table 3), indicating superiority of 2% rebamipide over 0.1% sodium hyaluronate. At all estimations (week 2, week 4, and LOCF), the improvements in FCS and LGCS scores were significantly greater for 2% rebamipide than for 0.1% sodium hyaluronate.

In the 34 patients with Sjögren's syndrome (17 patients per each treatment group), there were no significant differences between the 2% rebamipide and 0.1% sodium hyaluronate groups in the change from baseline to LOCF in the FCS score (−3.4 vs. −2.5, respectively) and the LGCS score (−3.7 vs. −2.1, respectively). However, these scores in the 2% rebamipide group showed a tendency for better improvement compared with the 0.1% sodium hyaluronate group.

Secondary End Points. There were similar changes between treatment groups in the change from baseline to LOCF for Schirmer's test results or TBUT (Table 3). Changes from baseline to LOCF in the dry eye–related ocular symptoms of foreign body sensation and eye pain were significantly greater in the 2% rebamipide group than in the 0.1% sodium hyaluronate group (Table 3). There was no significant difference between groups for change from baseline to LOCF in dryness, photophobia, or blurred vision, although there were more improvements with 2% rebamipide.

The patients' overall treatment impression with 2% rebamipide was significantly more favorable than that with 0.1% sodium hyaluronate ($P<0.001$, Wilcoxon signed-rank test; Fig 2). Overall, 60 patients (64.5%) rated their symptoms as improved or markedly improved in the 2% rebamipide group, compared with 33 patients (34.7%) in the 0.1% sodium hyaluronate group.

Safety Evaluation

Adverse events were observed in 27 patients (29.0%) in the 2% rebamipide group and in 19 patients (20.0%) in the 0.1% sodium hyaluronate group. Adverse events observed in at least 2 patients are shown in Table 4. The most frequently observed adverse event was dysgeusia (bitter taste), which was observed only in the 2% rebamipide group (9 adverse events in 9 patients; 9.7%). All cases of dysgeusia reported in this study were judged to be treatment related. Dysgeusia and all eye disorders were mild in severity and resolved either with appropriate treatment or with no treatment. No deaths and no serious or severe adverse events were observed in this study. A total of 3 patients in the 0.1% sodium hyaluronate group and 1 patient in the 2% rebamipide group discontinued because of adverse events.

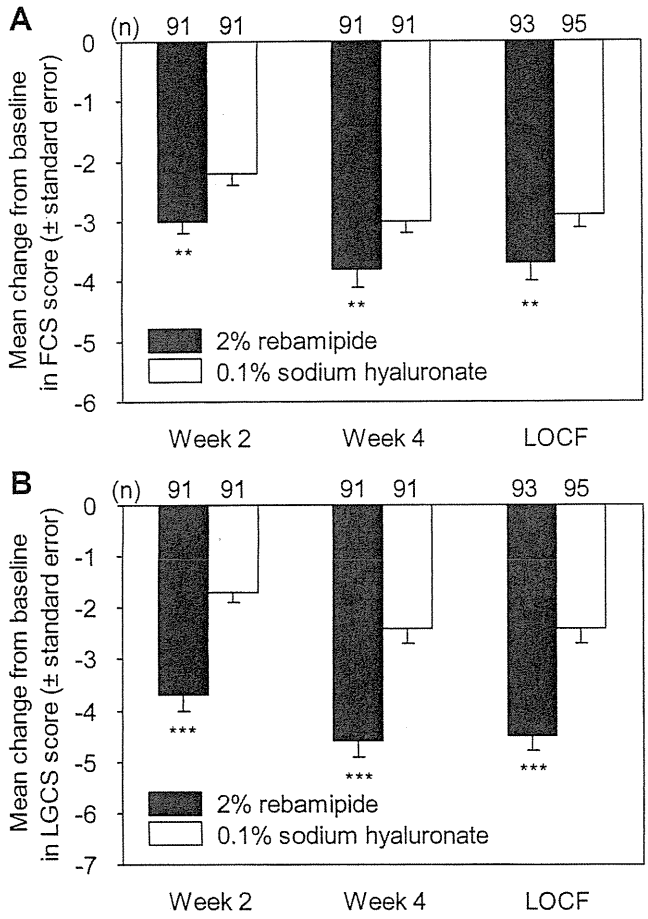

Figure 1. A, Change in fluorescein corneal staining (FCS) score from baseline to week 2, week 4, and last observation carried forward (LOCF); B, Change in lissamine green conjunctival staining (LGCS) score from baseline to week 2, week 4, and LOCF. $^{**}P<0.01$, $^{***}P<0.001$ vs 0.1% sodium hyaluronate (*t* test).

Discussion

In this phase 3 trial, rebamipide demonstrated statistically significant efficacy improvements over sodium hyaluronate for the treatment of dry eye. The 4-week, 4-times daily ocular instillation of 2% rebamipide was effective at improving both the objective signs and the subjective symptoms of dry eye. Study data were obtained from a population representative of that seen in normal clinical practice, because dry eye commonly affects women who are middle-aged and older.[27,28] Results from this study support and confirm the data from the phase 2 trial, which reported significant benefits of 2% rebamipide over the placebo.[24] Furthermore, rebamipide again demonstrated its rapid onset of effect (2 weeks).

In the primary analysis, in relation to the change from baseline in both FCS and LGCS scores, 2% rebamipide clearly demonstrated a marked improvement. Such improvements in staining scores are important because they indicate an improvement in the ocular surface,[2] with FCS reflecting corneal epithelium integrity and LGCS reflecting conjunctival epithelium integrity. Staining with fluorescein and lissamine green are the standard methods used to demonstrate ocular surface damage.[2,29] Patients with Sjögren's syndrome may have a particularly severe form of dry eye. Subgroup analysis of the 34 patients with Sjögren's syndrome in this study showed a tendency for better improvement for 2% rebamipide over 0.1% sodium hyaluronate on the primary end points. This tendency suggests the potential use of 2% rebamipide for dry eye in patients with Sjögren's syndrome.

In addition to its benefits on objective measures, 2% rebamipide was more effective than 0.1% sodium hyaluronate on subjective outcomes, showing greater improvement in symptoms. Significantly greater improvements in foreign body sensation and eye pain were seen with 2% rebamipide compared with 0.1% sodium hyaluronate. The assessment of efficacy using subjective measures (symptoms) as well as objective measures (signs) is particularly important in patients with dry eye because it has been shown that there is poor correlation between symptoms and signs of dry eye; for instance, one study found that only 57% of symptomatic patients were shown to have objective signs of dry eye.[30] Improvements in symptoms are important, given the impact of dry eye on quality of life.[2,5]

Rebamipide has distinctive features compared with other drugs that are used in current therapies for dry eye. Cyclosporine, another ophthalmic solution used for the treatment of dry eye, showed significant improvement in FCS score, although efficacy was demonstrated only after 4 months.[31] Sodium hyaluronate also has shown effectiveness in patients with dry eye, with FCS scores demonstrating significant improvement at 4 weeks.[7] In addition, FCS scores also showed significant improvement at 2 weeks compared with baseline scores.[8] In the present study, rebamipide demonstrated better efficacy after 2 weeks of treatment compared with sodium hyaluronate. Cyclosporine has an anti-inflammatory and immunomodulatory mode of action, and sodium hyaluronate is a viscous material aimed at increasing tear retention and wound healing effects. In contrast, rebamipide has been shown to increase the number of periodic acid–Schiff-positive cells (goblet cells) in the conjunctiva[22] and the mucin level on the cornea and conjunctiva.[22,23] Because decreased mucin levels on the surface of the cornea and a decreased density of goblet cells have been observed in patients with dry eye,[32] the method of action of rebamipide is expected to be beneficial for this disease. With this mechanism in mind, rebamipide also is expected to be effective in patients with dry eye resulting from short

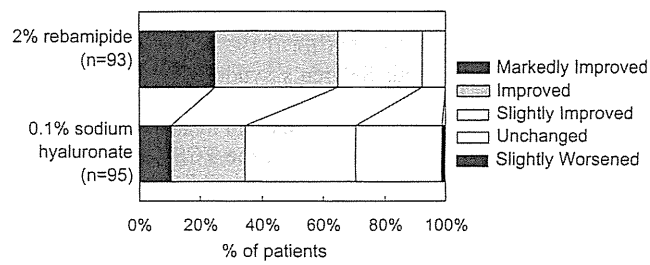

Figure 2. Patient's overall treatment impression by category. No patients responded worsened or markedly worsened in any treatment group.